Chap.6 Formation and evolution of Local Group galaxies

- Properties of Local Group galaxies
- New aspects of Magellanic Clouds
- Formation of satellite galaxies
- New insights into the missing satellites problem
- Formation of the Andromeda galaxy

6.1 Properties of Local Group galaxies

Milky Way and satellite galaxies

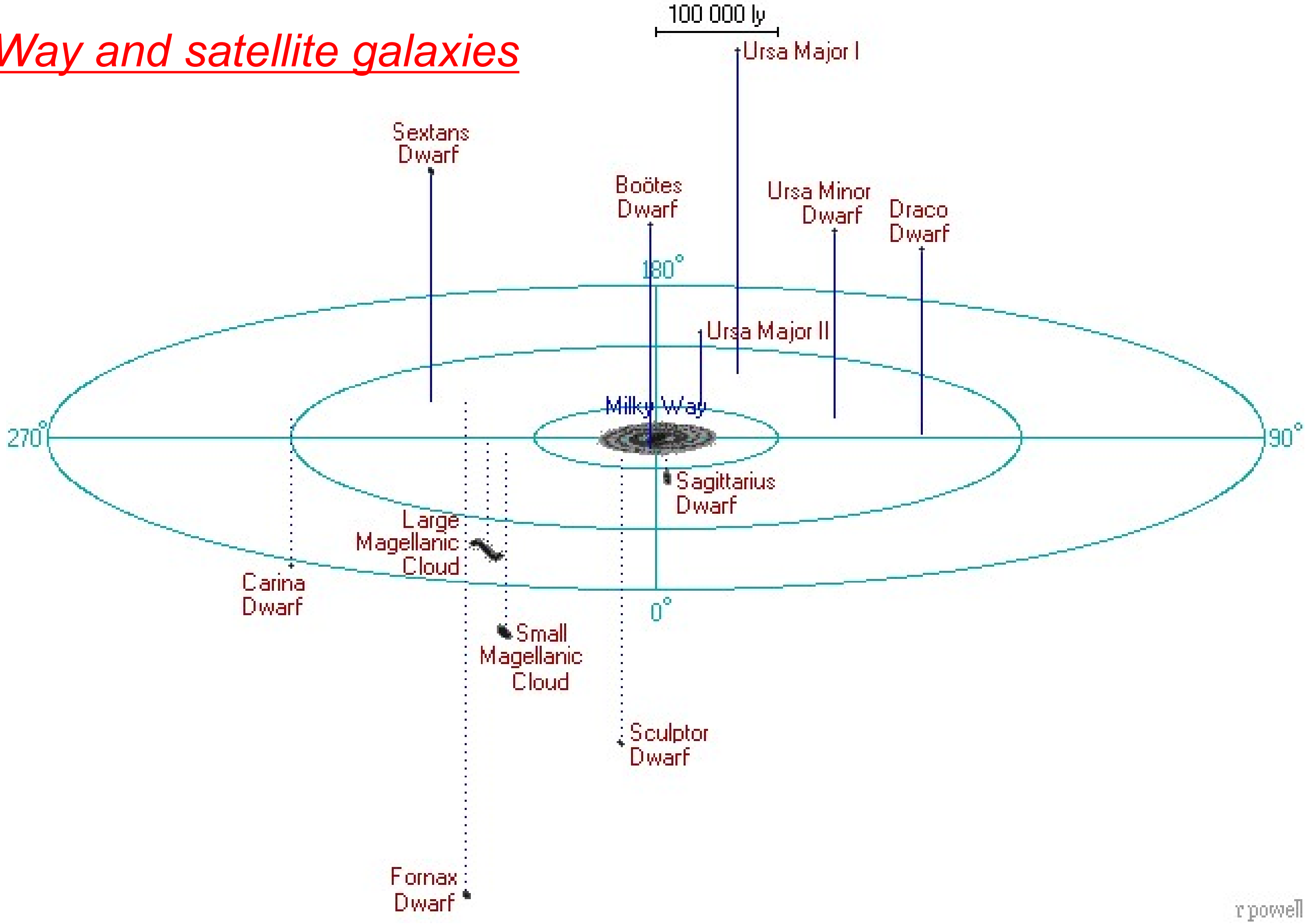

Local Group

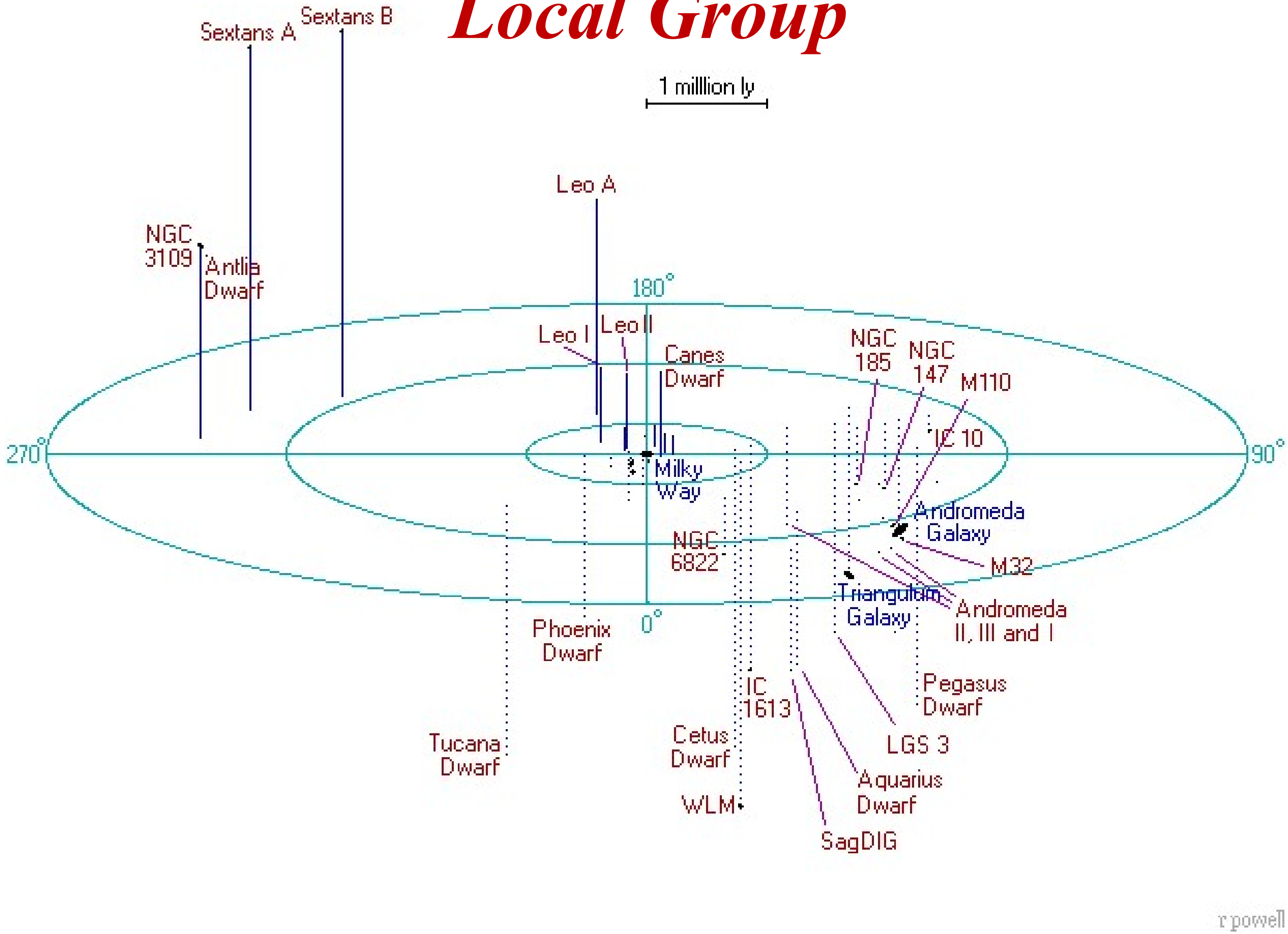

1 milllion ly
Sextans A
Sextans B
Leo A
NGC 3109
Antlia Dwarf
180°
270°
90°
0°
Leo I
Leo II
Canes Dwarf
NGC 185
NGC 147
M110
IC 10
Milky Way
Andromeda Galaxy
NGC 6822
M32
Triangulum Galaxy
Andromeda II, III and I
Phoenix Dwarf
IC 1613
Pegasus Dwarf
LGS 3
Tucana Dwarf
Cetus Dwarf
Aquarius Dwarf
WLM
SagDIG
r powell

	Name	Type	l [deg]	b [deg]	$D_{\odot}$ [kpc]	$D_{\rm LG}$ [Mpc]	M_V [mag]	μ_V [mag/"^{2}]	$\langle$[Fe/H]$\rangle$ [dex]
MW	Galaxy	S(B)bcI-II	0.00	0.00	8	0.47	−20.9	—	—
	Sgr	dSph,N?	6.00	−15.00	28	0.47	−13.8	25.4	−1.0
	LMC	IrIII-IV	280.46	−32.89	50	0.49	−18.5	20.7	−0.7
	SMC	IrIV/IV-V	302.80	−44.30	63	0.49	−17.1	22.1	−1.0
	UMi	dSph	104.95	44.80	69	0.44	−8.9	25.5	−2.2
	Dra	dSph	86.37	34.72	79	0.44	−8.6	25.3	−2.1
	Sex	dSph	243.50	42.27	86	0.52	−9.5	26.2	−1.7
	Scl	dSph	287.54	−83.16	88	0.45	−9.8	23.7	−1.8
	Car	dSph	260.11	−22.22	94	0.52	−9.4	25.5	−2.0
	For	dSph	237.29	−65.65	138	0.46	−13.1	23.4	−1.3
	Leo II	dSph	220.17	67.23	205	0.57	−10.1	24.0	−1.9
	Leo I	dSph	225.98	49.11	270	0.63	−11.9	22.4	−1.5
	Phe	dIrr/dSph	272.49	−68.82	405	0.60	−9.8	—	−1.8
	NGC 6822	IrIV-V	25.34	−18.39	500	0.68	−16.0	21.4	−1.2
M31	M31	SbI-II	121.18	−21.57	770	0.31	−21.2	10.8	—
	M32	dE2,N	121.15	−21.98	770	0.31	−16.5	11.5	−1.1
	NGC 205	dE5p,N	120.72	−21.14	830	0.37	−16.4	20.4	−0.5
	And I	dSph	121.69	−24.85	790	0.33	−11.8	24.9	−1.5
	And III	dSph	119.31	−26.25	760	0.30	−10.2	25.3	−1.5
	NGC 147	dE5	119.82	−14.25	755	0.30	−15.1	21.6	−1.1
	And V	dSph	126.20	−15.10	810	0.36	−9.1	24.8	−1.9
	And II	dSph	128.87	−29.17	680	0.24	−11.8	24.8	−1.5
	NGC 185	dE3p	120.79	−14.48	620	0.17	−15.6	20.1	−0.8
	M33	ScII-III	133.61	−31.33	850	0.42	−18.9	10.7	—
	Cas dSph	dSph	109.46	−9.94	760	0.34	−12.0	23.5	−1.6
	IC 10	IrIV:	118.97	−3.34	660	0.26	−16.3	22.1	−1.3:
	And VI	dSph	106.01	−36.30	775	0.38	−11.3	24.3	−1.9
	LGS 3	dIrr/dSph	126.75	−40.90	810	0.41	−10.5	24.7	−2.2
	Peg	IrV	94.77	−43.55	760	0.44	−12.3	—	−1.3
	IC 1613	IrV	129.82	−60.54	715	0.47	−15.3	22.8	−1.4
isolated	Cet	dSph	101.50	−72.90	775	0.62	−10.1	25.1	−1.9
	Leo A	IrV	196.90	52.40	690	0.88	−11.5	—	−1.7
	WLM	IrIV-V	75.85	−73.63	945	0.80	−14.4	20.4	−1.4
	Tuc	dSph	322.91	−47.37	870	1.11	−9.6	25.1	−1.7
	DDO 210	IrV	34.05	−31.35	950	0.96	−10.9	23.0	−1.9

Dwarf galaxies

dwarf spheroidal galaxies
（dSphs 矮小楕円体銀河）

Leo I

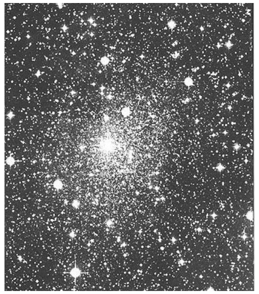

Carina

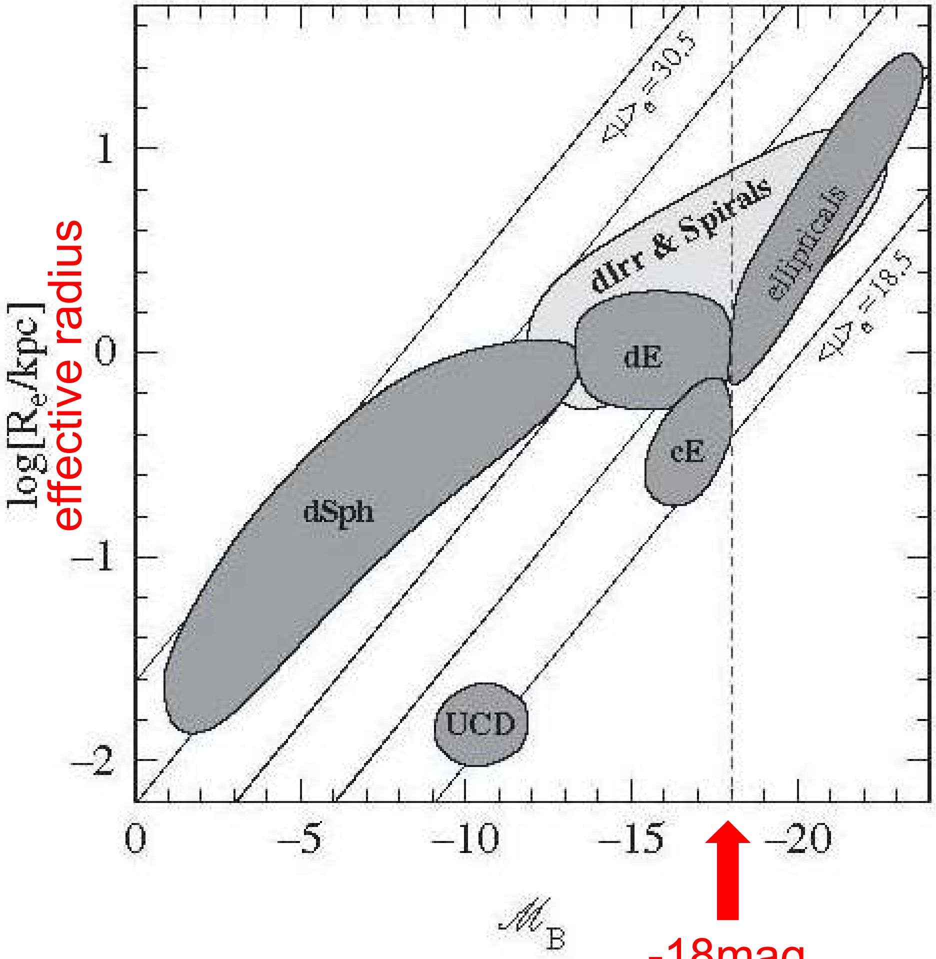

Structures of various types of galaxies

(Tolstoy+09, ARAA, 47, 371)

Classical dwarf satellites M_V < -8 mag
Ultra Faint Dwarfs (UFDs) M_V > -8 mag

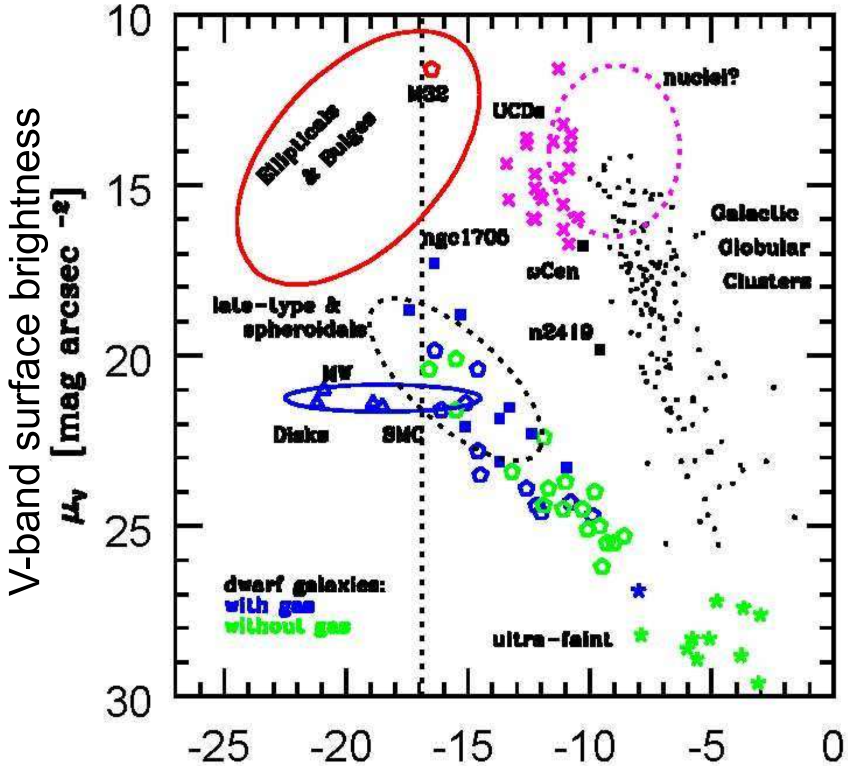

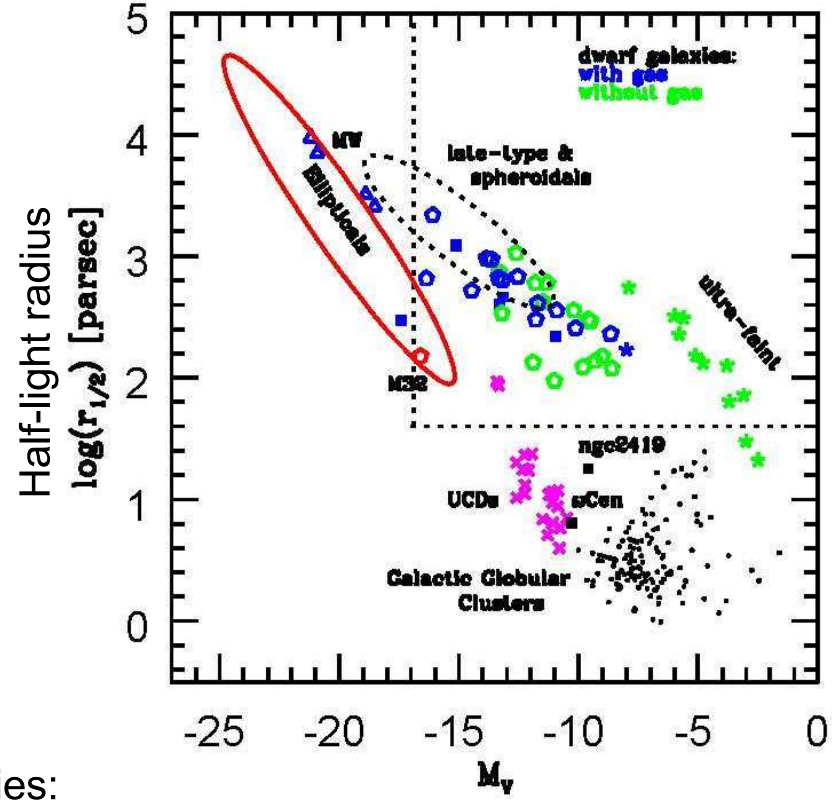

dwarf galaxies:
Mv > -17 and more spatially extended than globular clusters
with gas: dIrr, without gas: dSph

6.2 New aspects of Magellanic Clouds

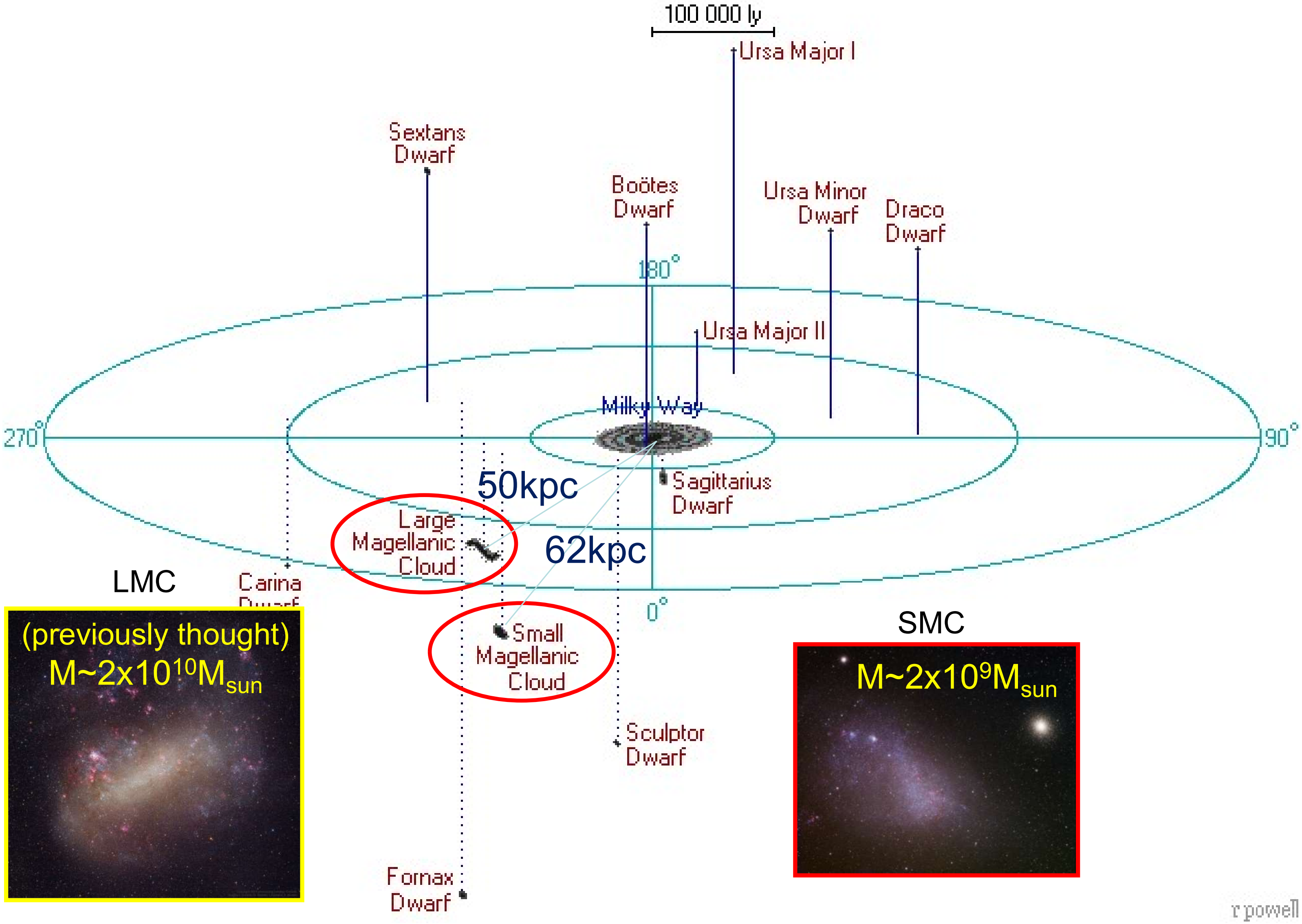

Most likely orbit of LMC/SMC to reproduce Magellanic Stream

(Diaz & Bekki 2012)

At least 2 pericentric passages over the past 4Gyrs

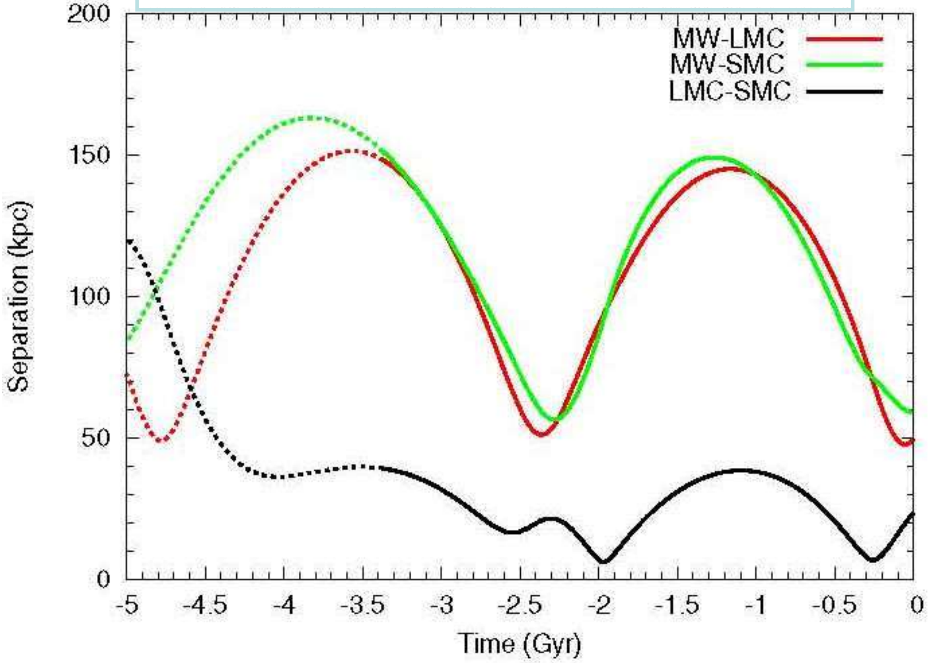

Magellanic Stream (HI)

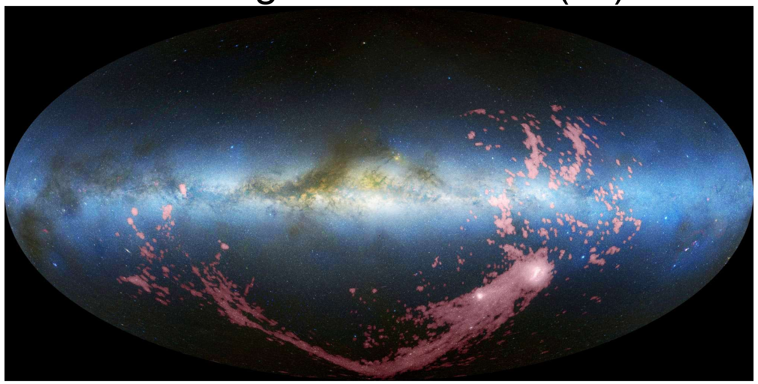

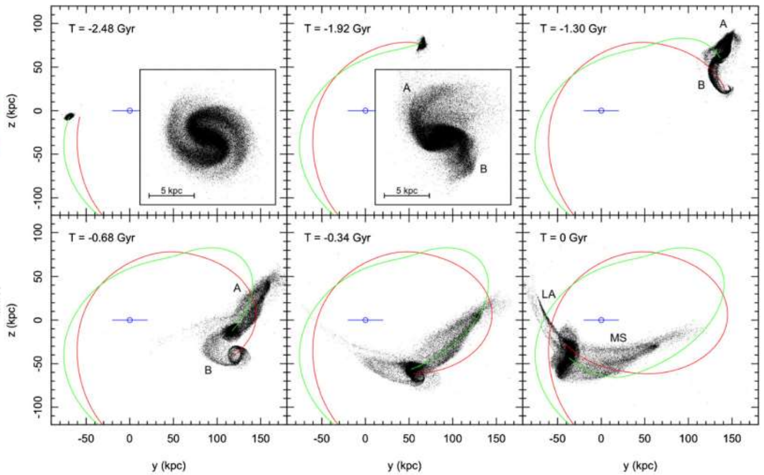

LMC/SMC's orbit

Recent several works (Gaia, HST) suggest the first infall of LMC/SMC

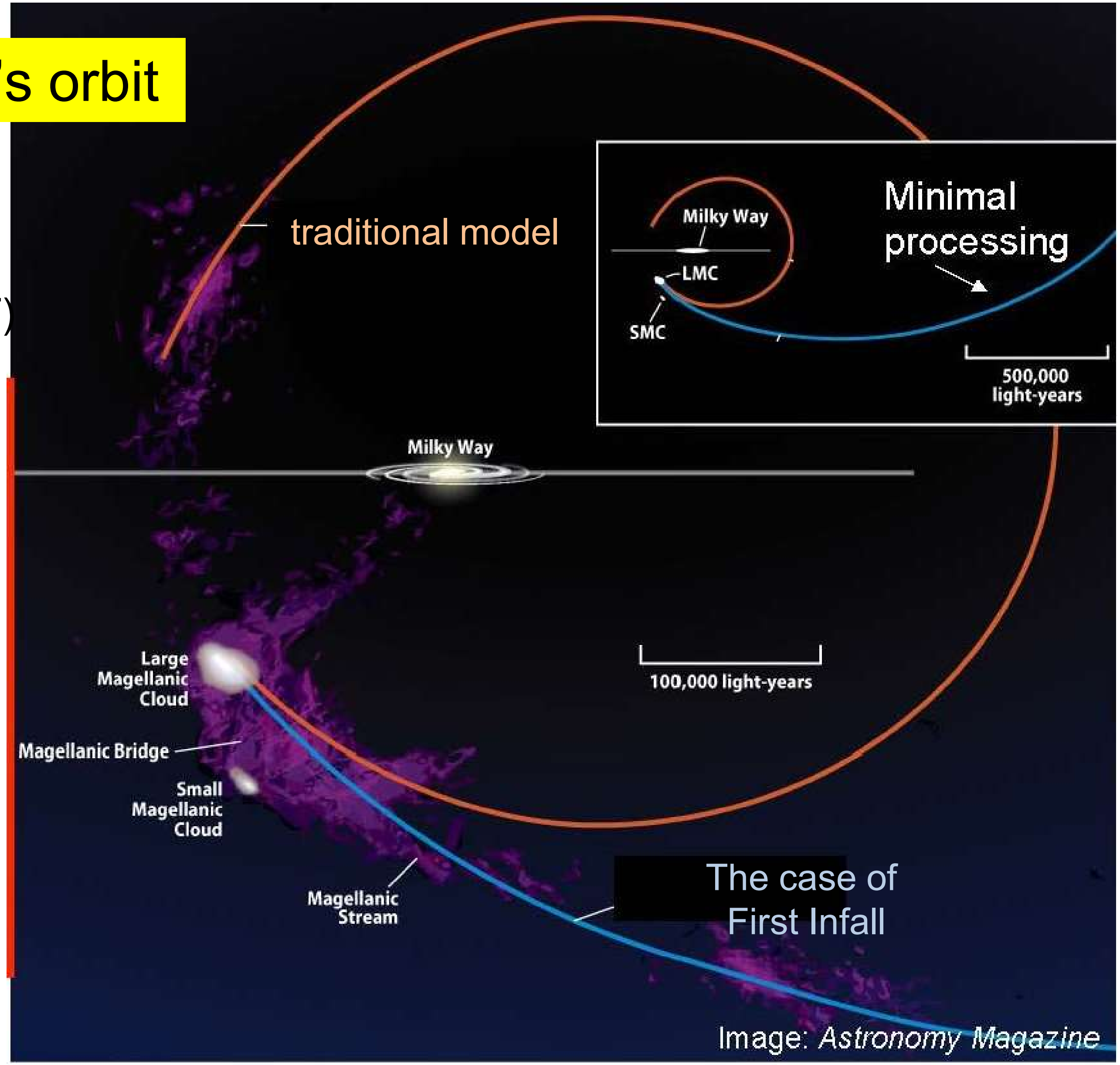

Besla+ 2010

Likely orbits of LMC/SMC + satellites using Gaia DR2: Patel et al. (2020)

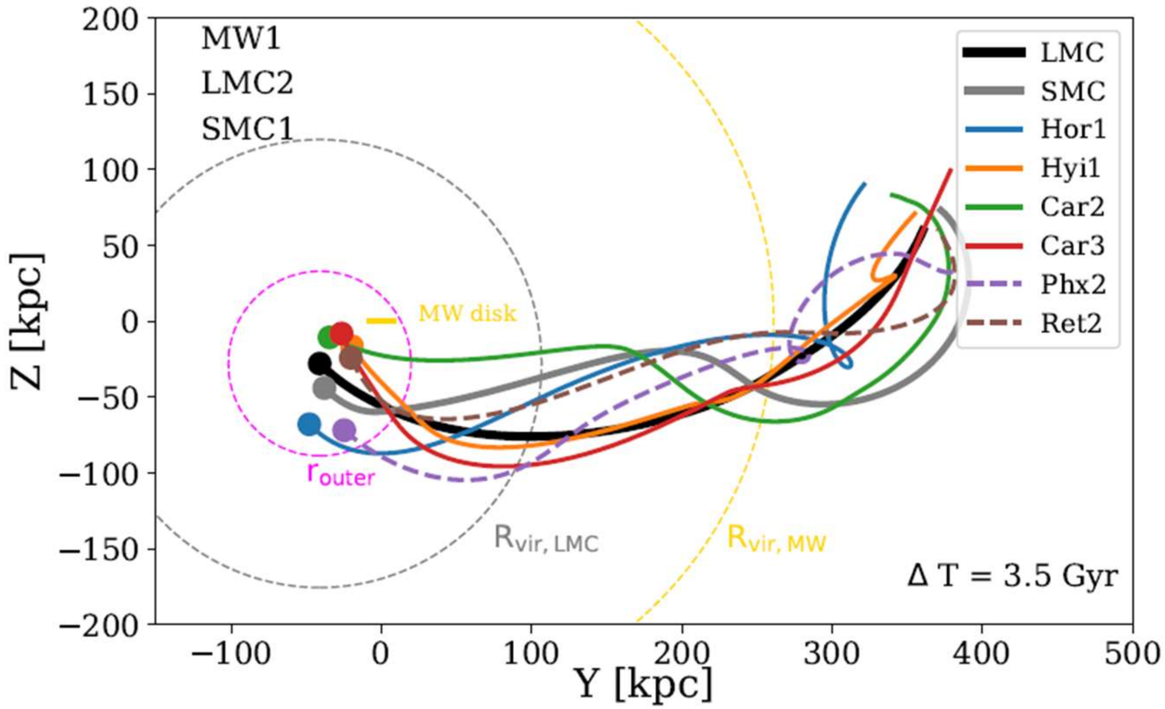

Figure 6. Direct orbits of all Magellanic satellites for the last 3.5 Gyr projected in the YZ-galactocentric plane. Recently captured Magellanic satellites (Ret2, Phx2) are illustrated with dashed lines and long-term Magellanic satellites (Car2, Car3, Hor1, Hyi1) are plotted with solid lines for MW1 using the fiducial LMC model. The disk of the MW lies along the z-axis. The orbit of the LMC (SMC) is illustrated in black (gray). The filled circles represent the positions of all satellites today. The magenta dashed circle indicates r_{outer} of the LMC and the gray dashed circle is the virial radius of the LMC. The gold dashed circle is the virial radius of the MW. The orbits of all Magellanic satellites follow the orbital path of the LMC.

Misaligned Orphan Stream
~effect of the very massive LMC?~

Erkal et al. 2019 (using Gaia DR2 PMs)

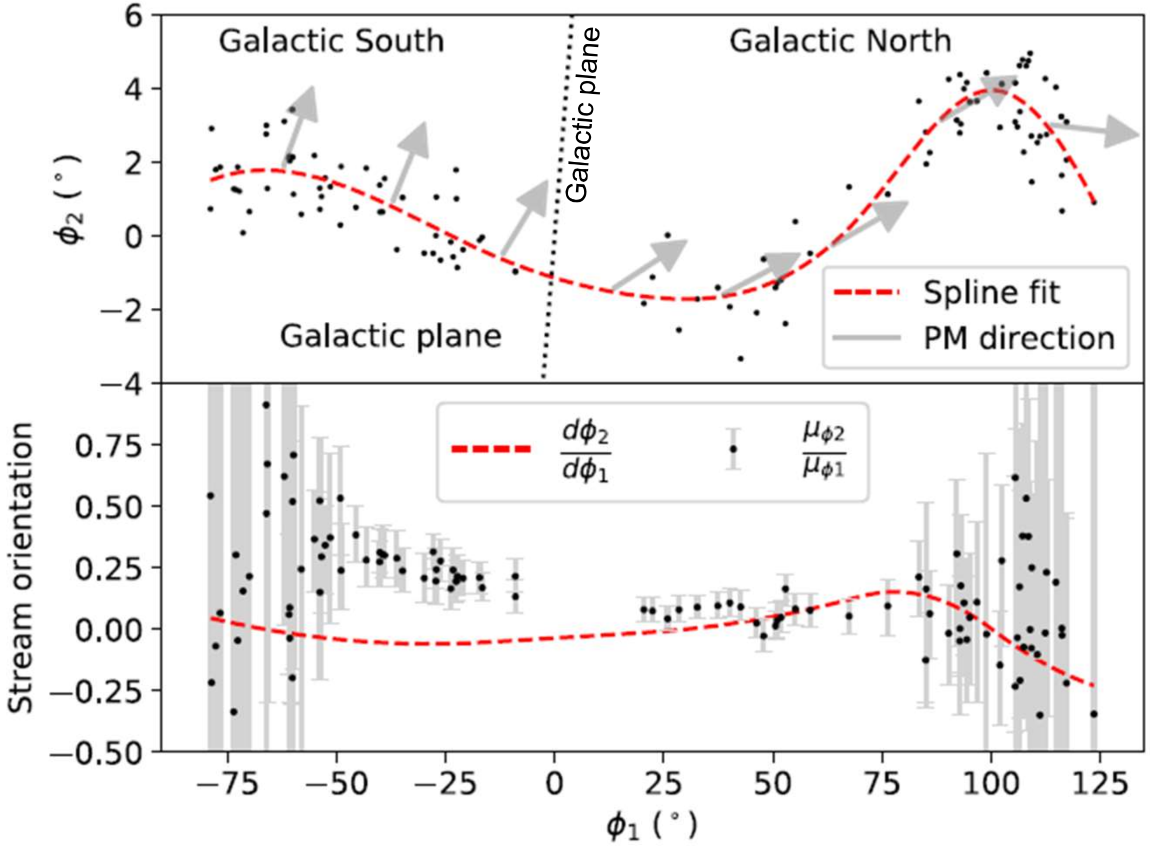

Points:
RR Lyrae
along OS

“Field of Streams” and new satellites in SDSS data (Belokurov et al. 2006)

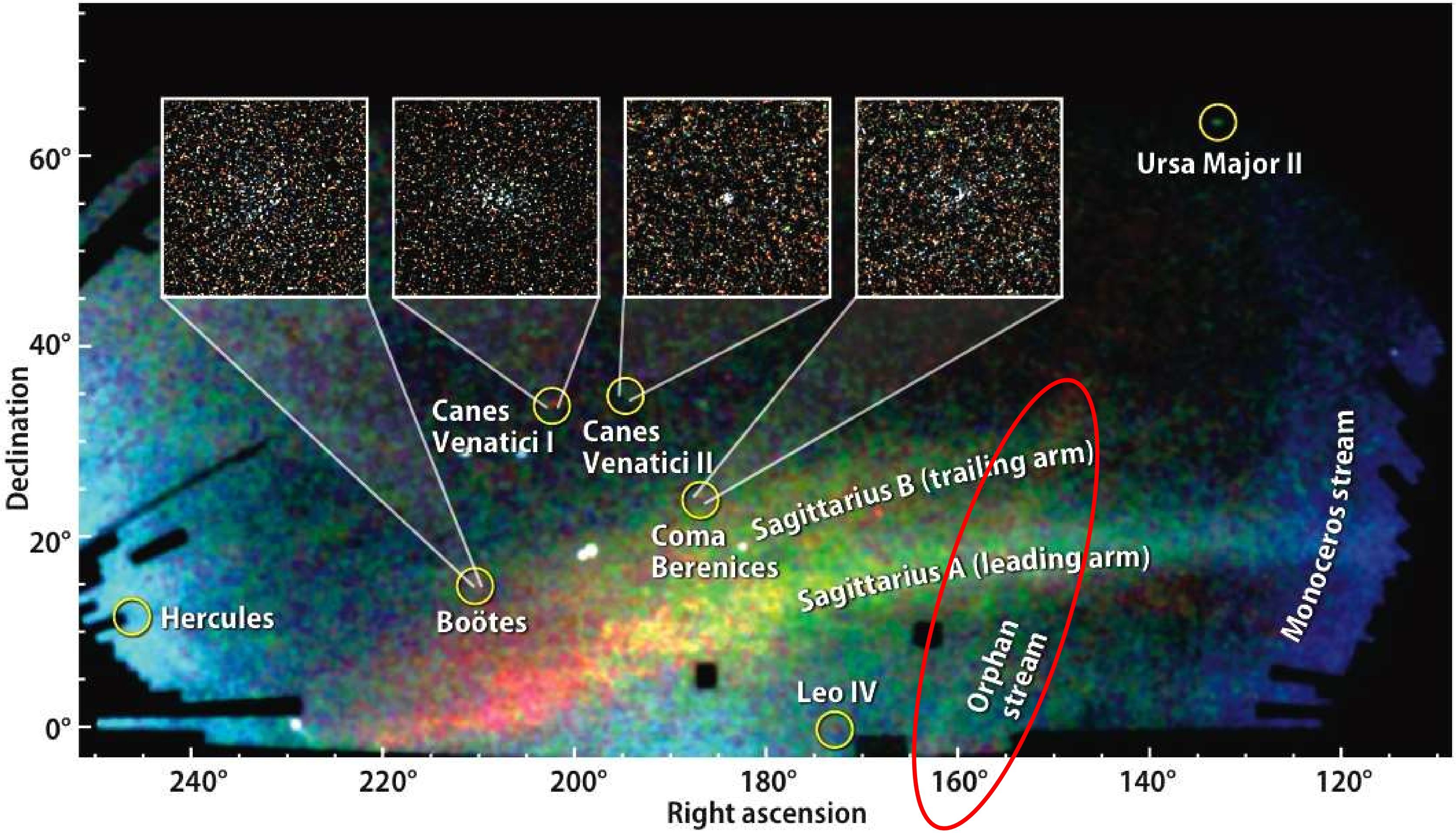

Misaligned Orphan Stream
~effect of the very massive LMC?~

Erkal et al. 2019 (using Gaia DR2 PMs)

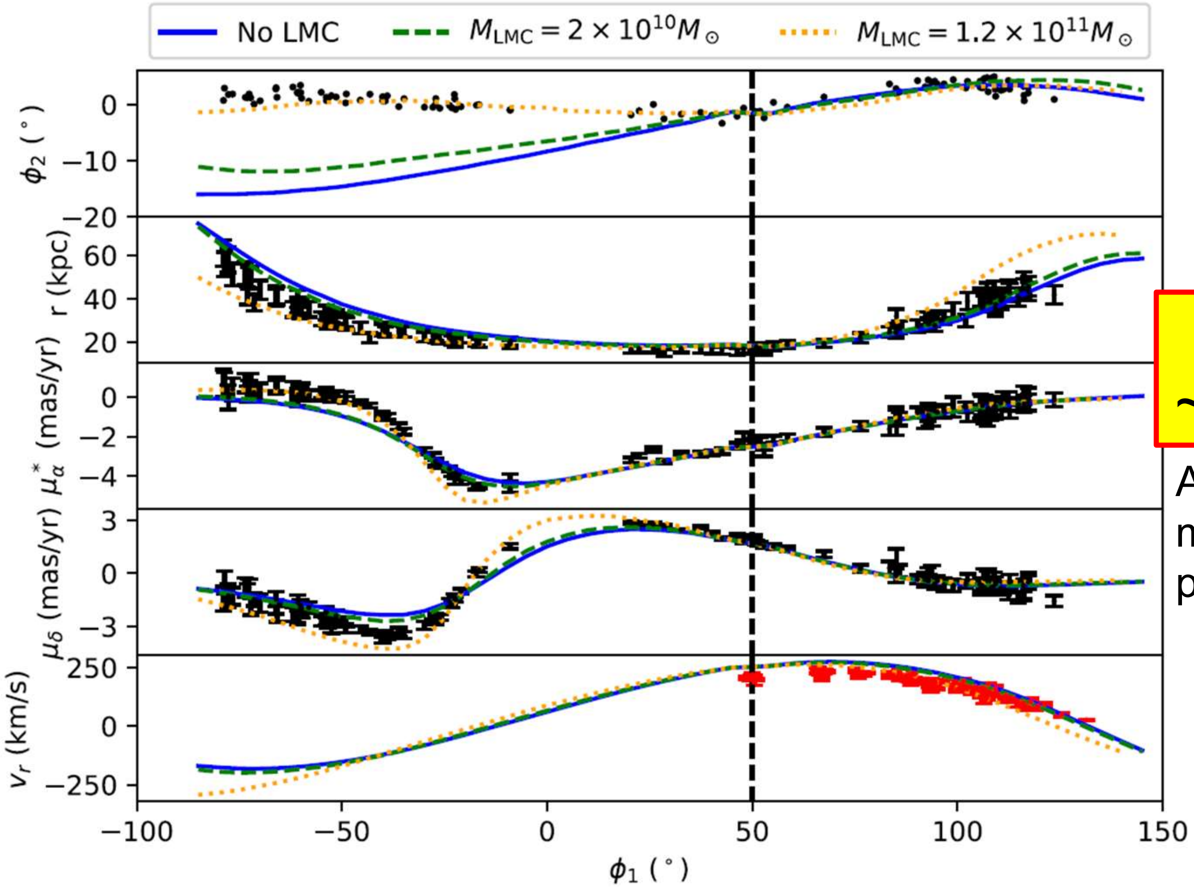

Best fit M_{LMC}
~ 1.38×10^{11} M_{sun}

An order of magnitude more massive than previously thought!

Wake effect of the massive LMC on MW's dark halo?

If $M_{LMC} \sim 10^{11}\ M_{sun}$
following recent results with Gaia

Effects on dark matter distribution in MW
(Garavito-Camargo et al. 2019)

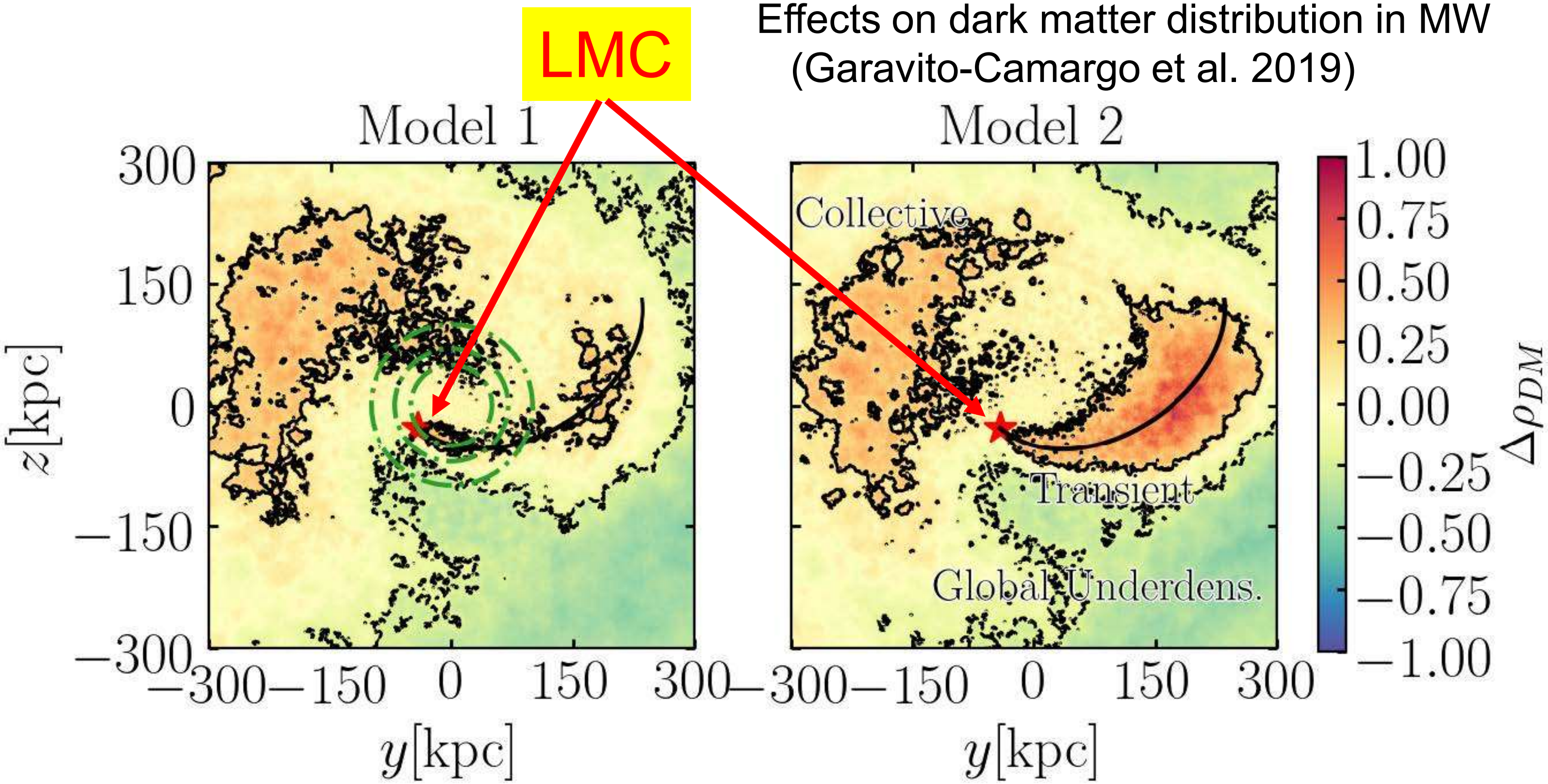

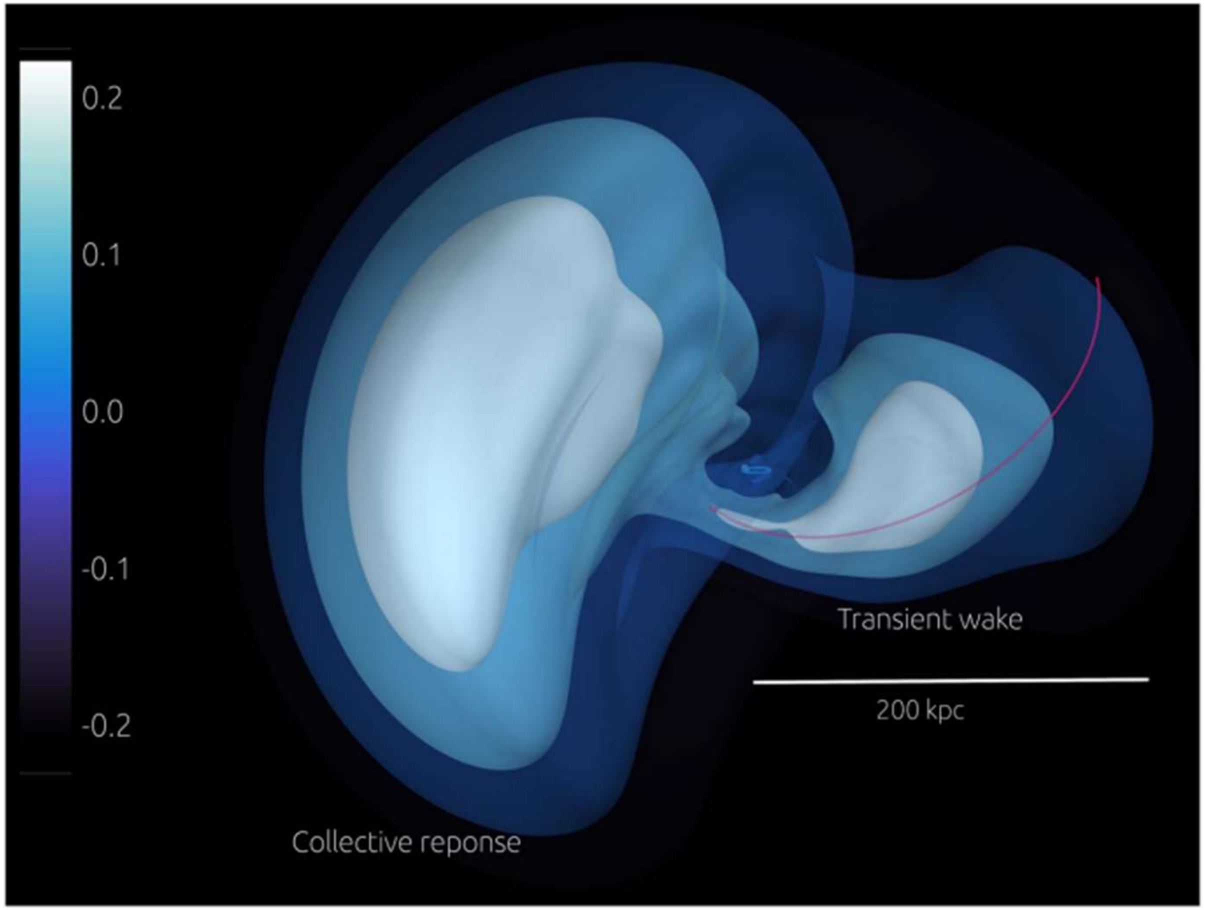

Figure 2. The LMC-induced DM dynamical friction wake and collective response in the MW DM halo at the present day, in the Galactocentric YZ plane. The den contours are computed using the BFE for the MW's DM halo. The color bar shows the density contrast as defined in Equation (6). White contours represent overdensities, while the darker blue contours show the underdensities. The dynamical friction wake is a large-scale structure ranging from ~50 kpc, near the LMC (red circle), out to the edge of the halo. The Collective Response is the larger overdensity that appears predominantly north of the MW disk (the latter is marked by the central blue ellipse). The Collective Response also appears to the south of the MW disk, at large distances. The red line marks the past passage of the LMC, which tracks the location of the dynamical friction wake. A 3D animated rendering of the density field of the MW illustrating the halo response to the LMC's passage, can be found on Vimeo https://vimeo.com/5462071170 and in the online Journal. The animated rendering rotates around the YZ plane, which is perpendicular to the galactic plane (XY).

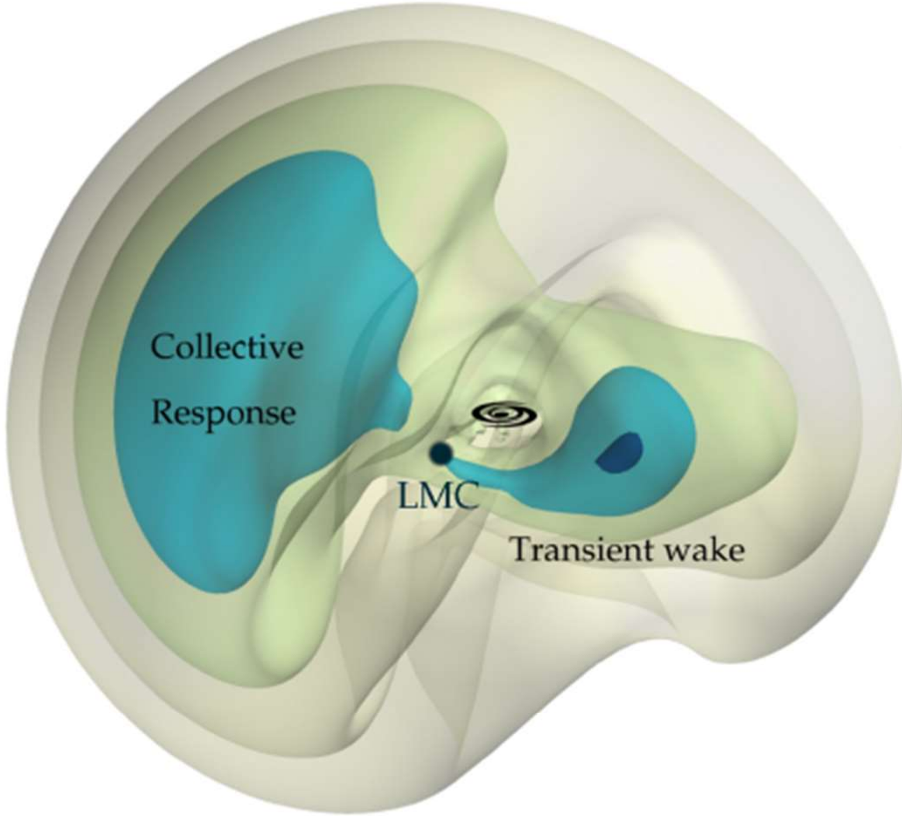

Garavito-Camargo et al. 2021

6.3 Formation of satellite galaxies

HST photometry of satellite galaxies

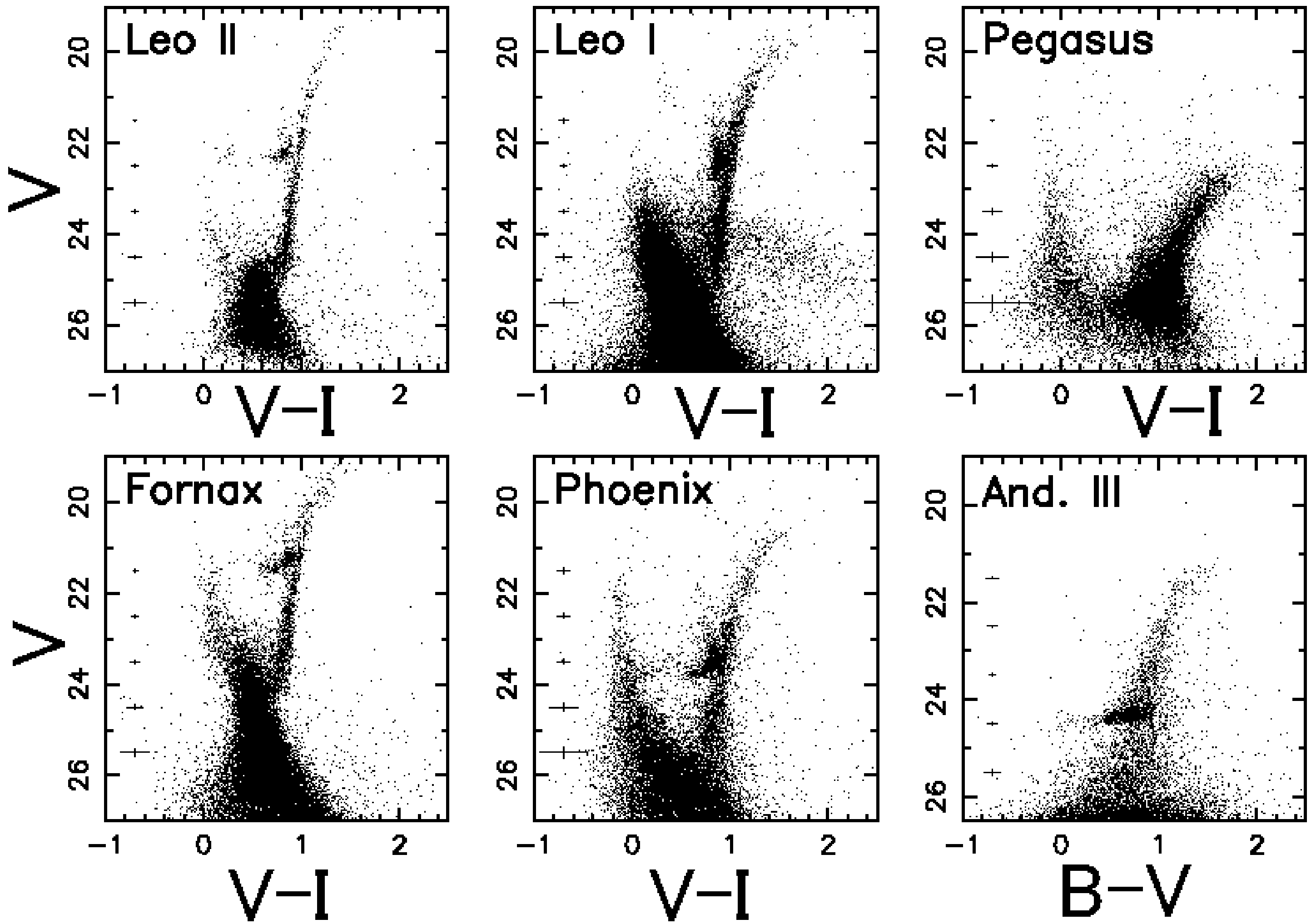

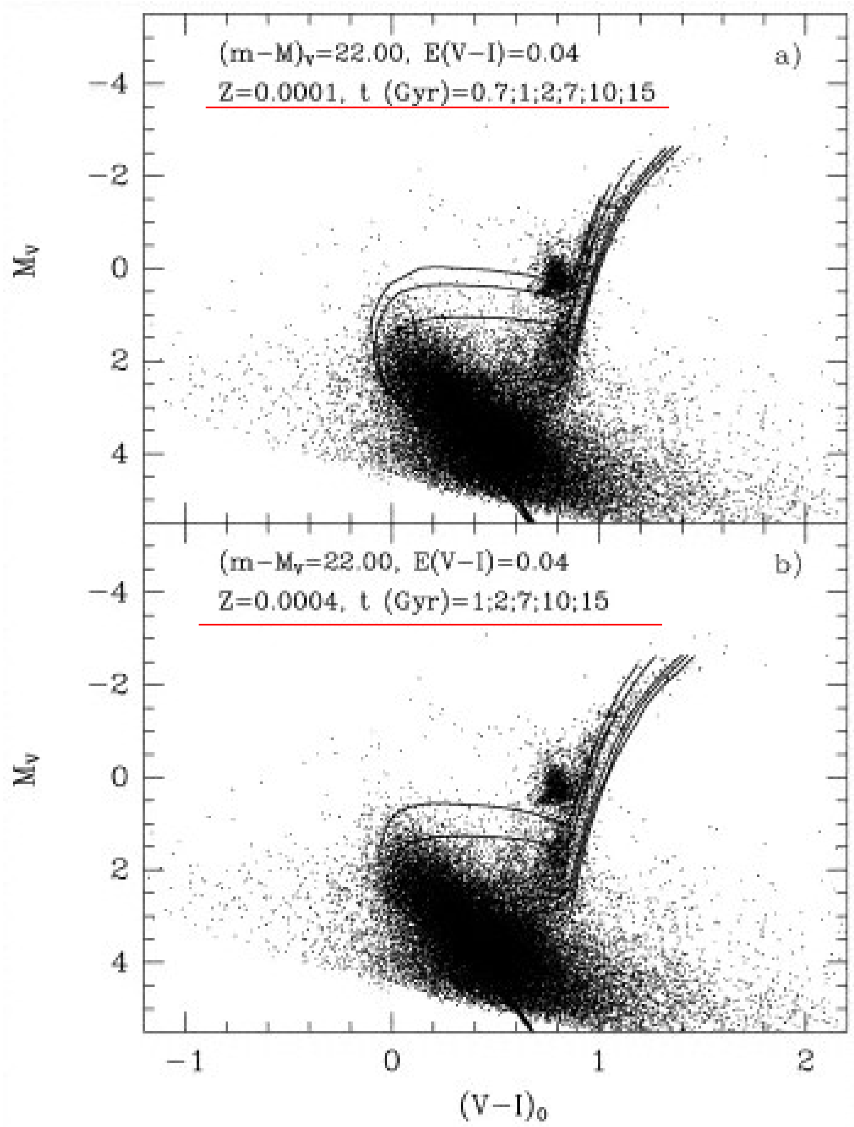

Leo I @ D=260kpc

Low SFR
lasting over ~10Gyr

Metallicity & Age
are degenerated

↓

Spectroscopy

Fornax @ D=138 kpc

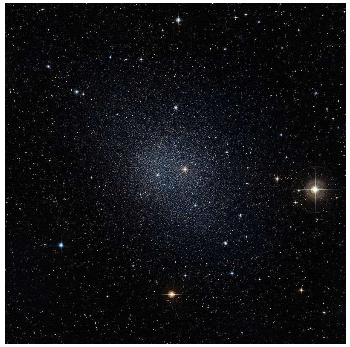

Buonanno+ 1999
(from HST image)

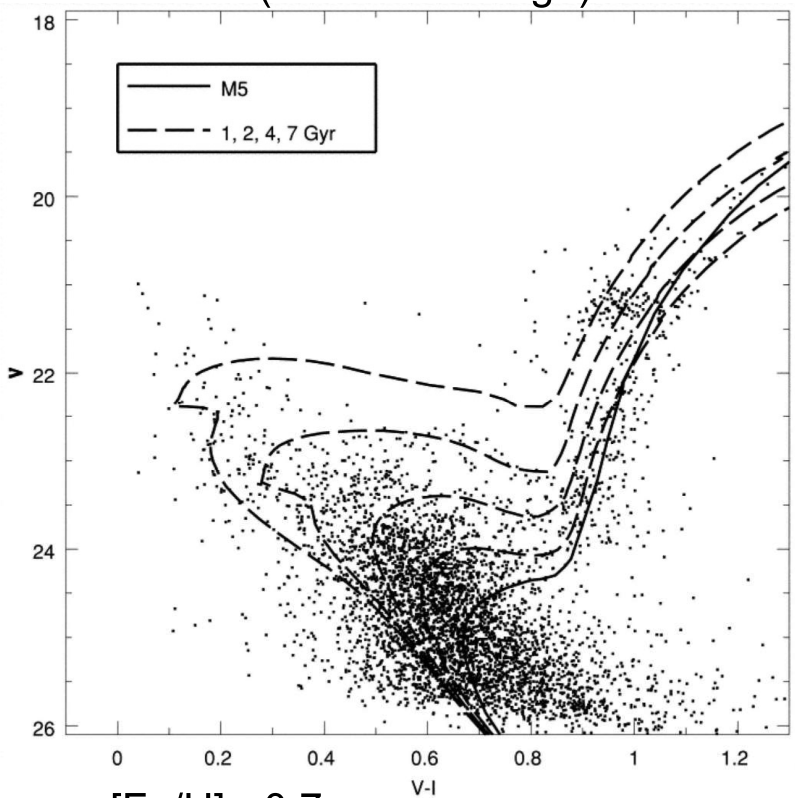

[Fe/H]=-0.7

de Boer+2012
(from CTIO image)

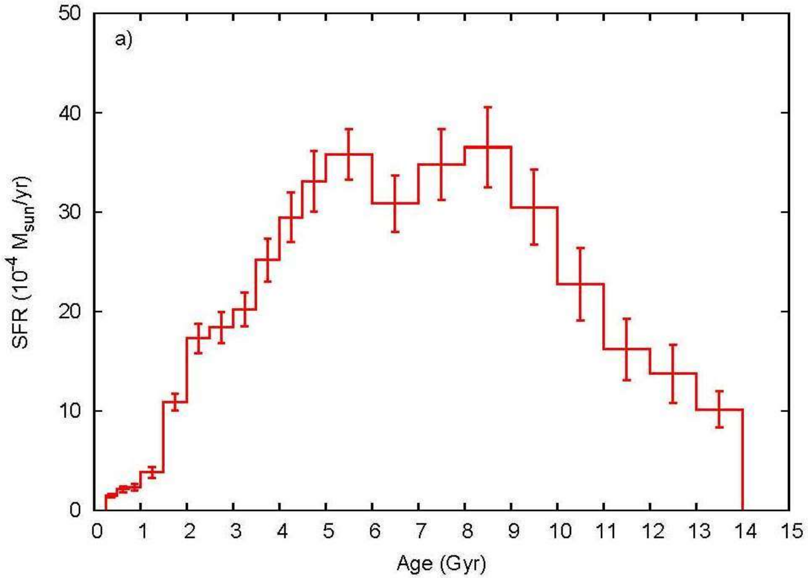

HST/WFPC2 results

(Weisz et al. 2014)

Varieties in SF histories

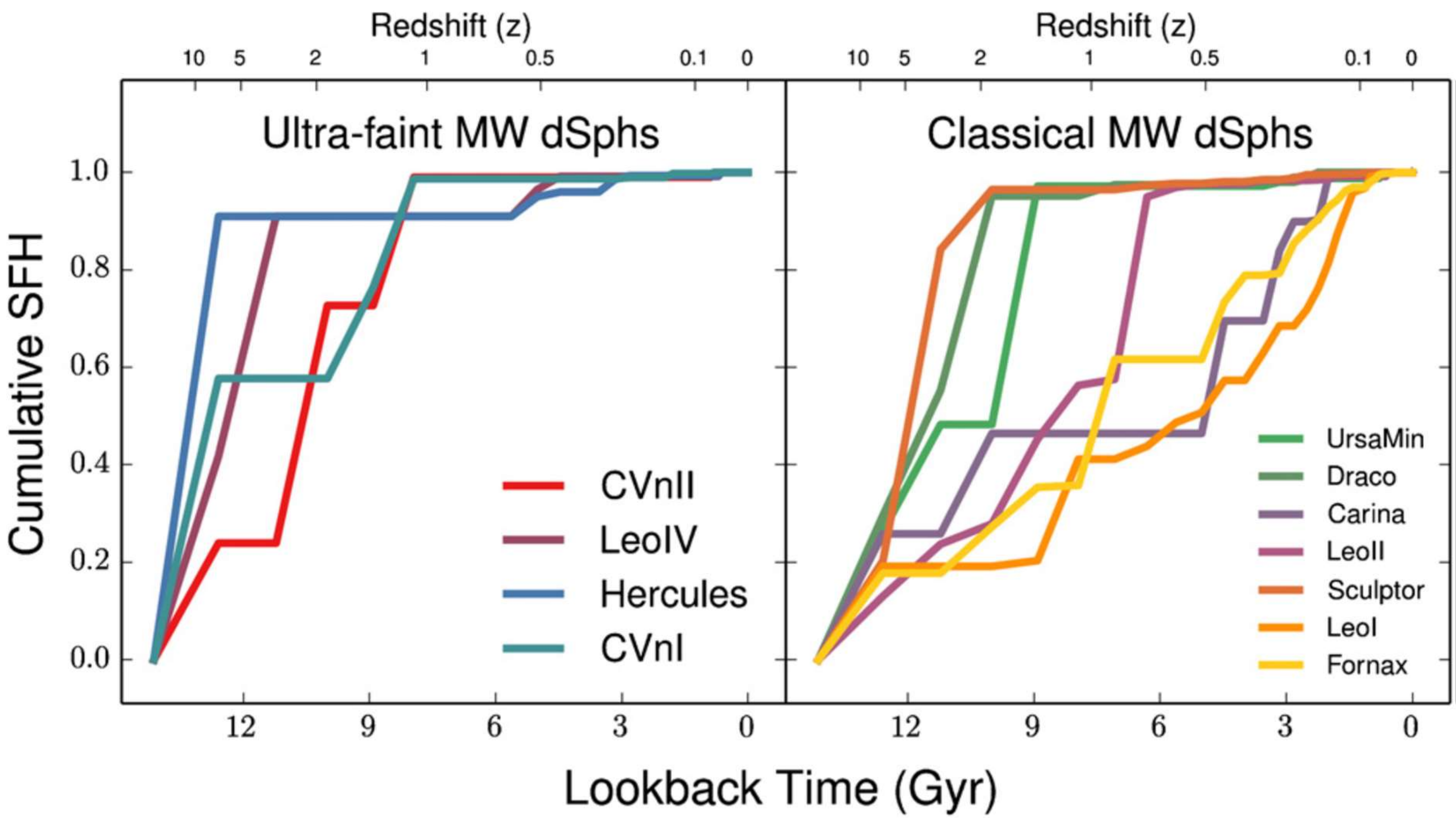

Long-term orbital motions of Galactic satellites in the growing mass of the Galactic halo
(Miyoshi & Chiba 2020)

Orbits using Gaia DR2

Classical dSphs ($M_V < -8$)

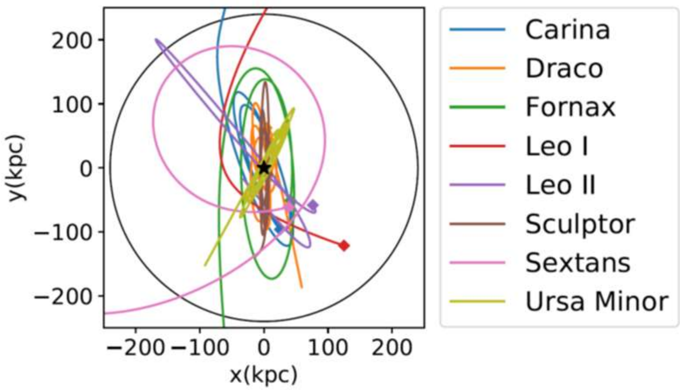

UFDs ($M_V > -8$)

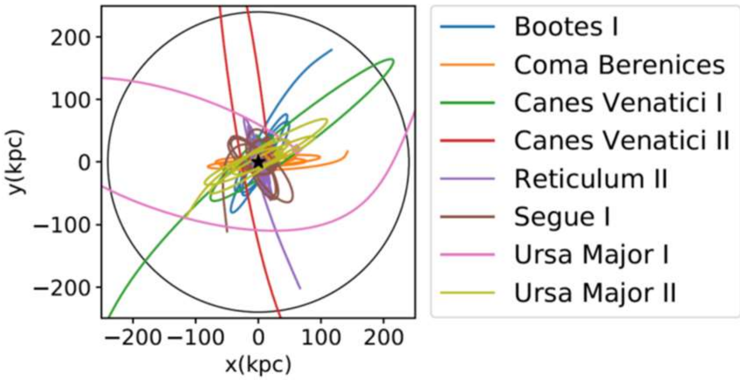

Draco

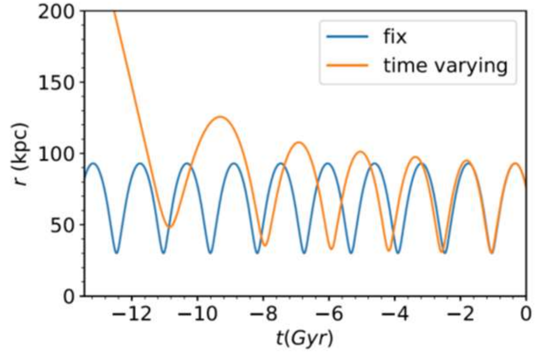

Look back time

Fornax

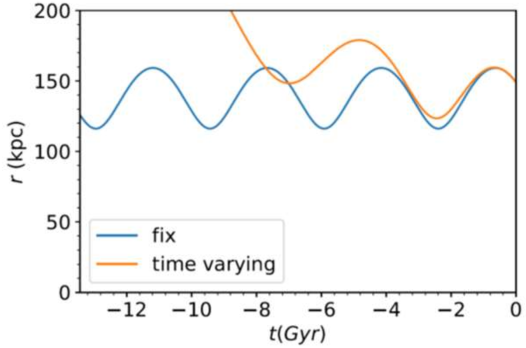

Look back time

Comparison between a fixed and evolving MW potential

(different at t > 4 Gyr)

Long-term orbital motions of Galactic satellites in the growing mass of the Galactic halo
(Miyoshi & Chiba 2020)

Classical dwarfs
($M_V < -8$)

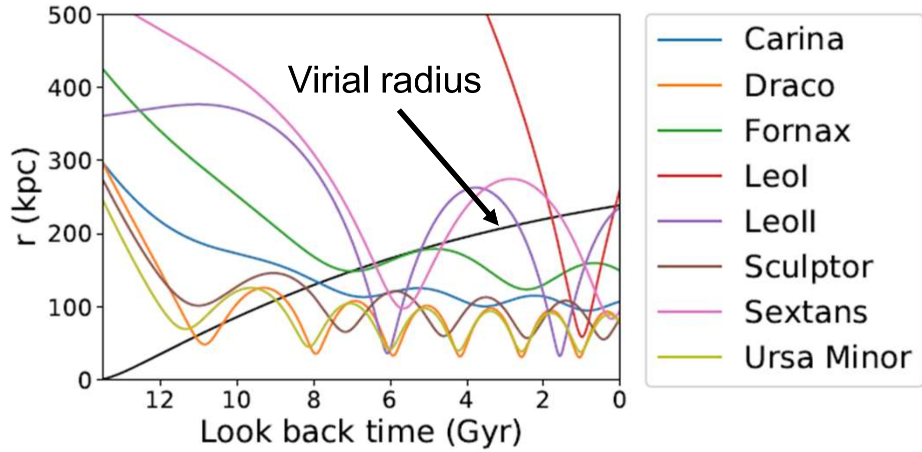

Ultra-faint dwarfs
(UFDs)
($M_V > -8$)

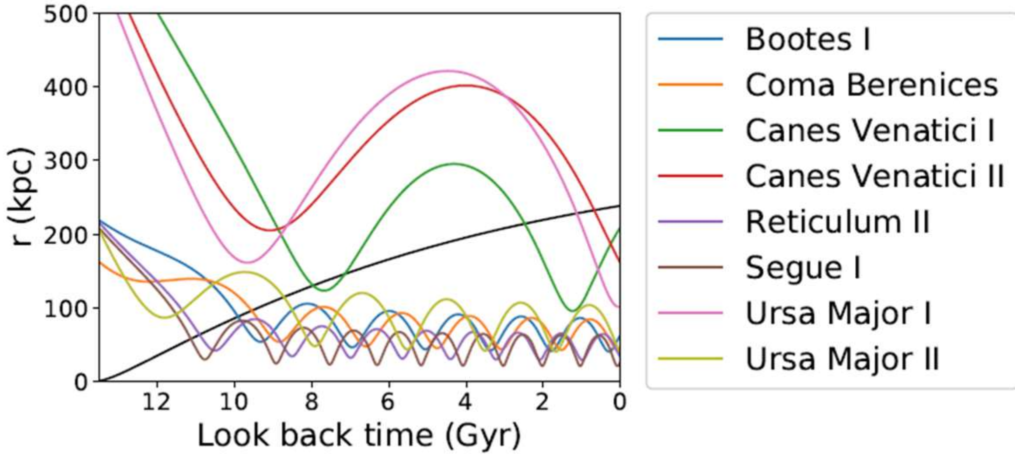

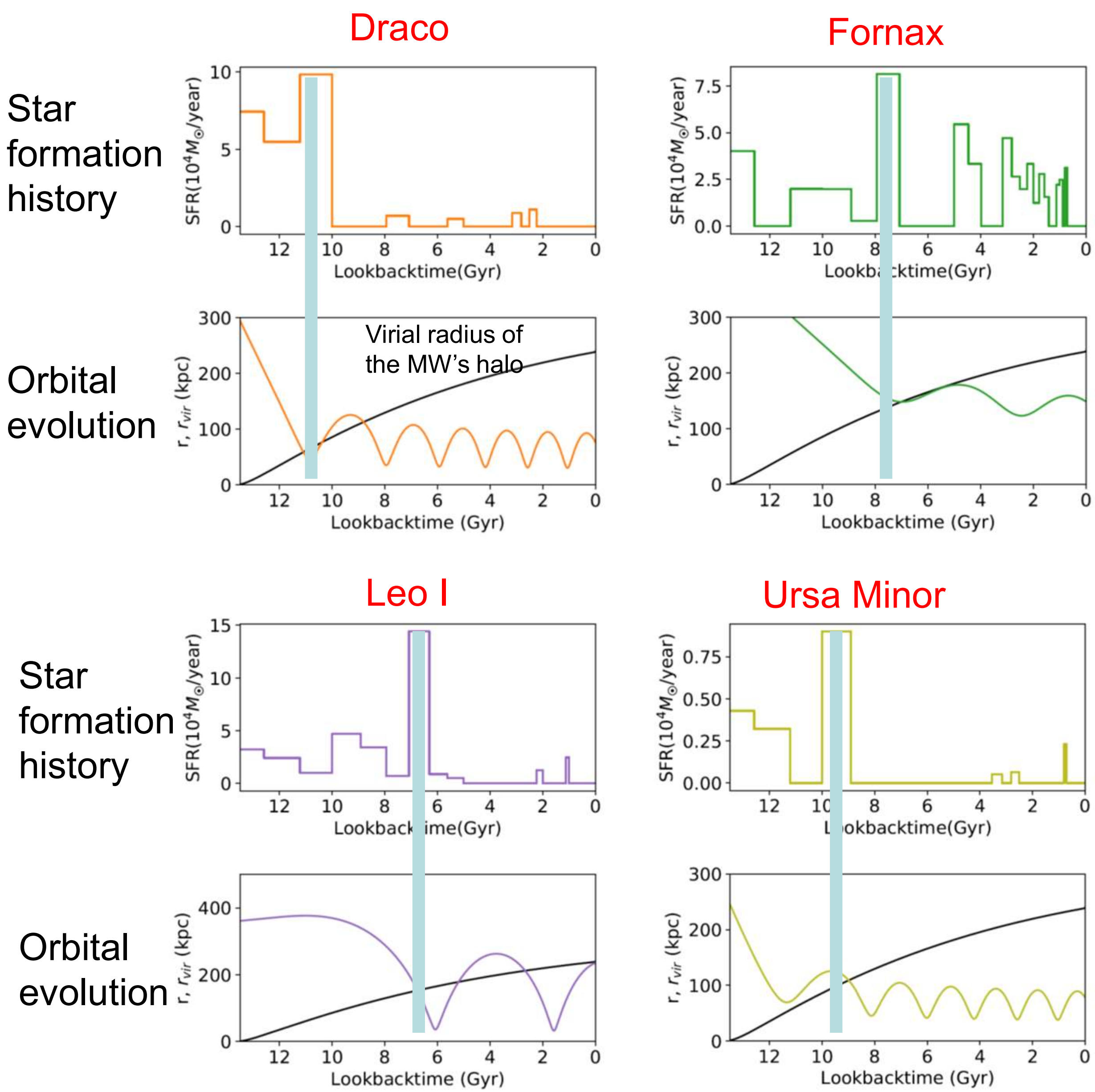

Miyoshi & Chiba 2020

First infall time crossing virial radius = time of SF peak (Star formation trigged by tidal effect + ram-pressure)

UFDs

Miyoshi & Chiba 2020

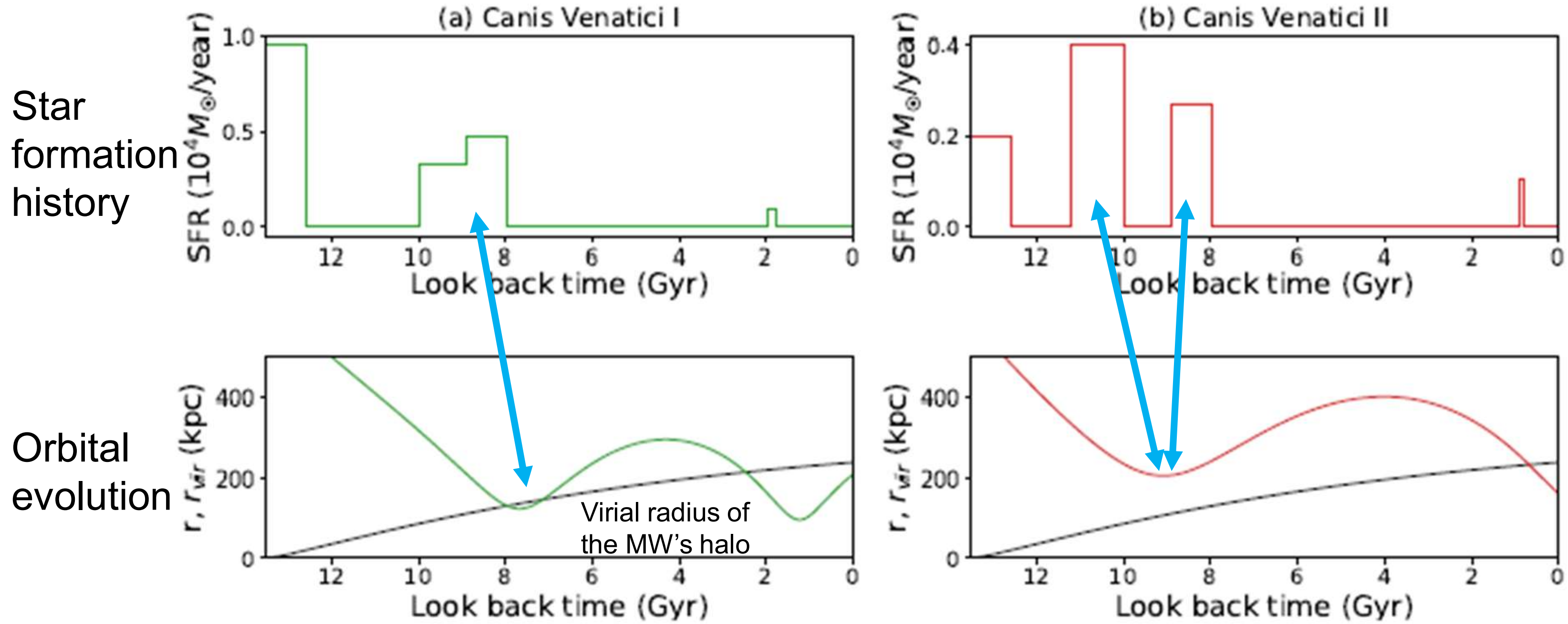

- 1st SF ended before the 1st infall and 2nd/3rd SF can be related to the infall
- What is the relation with r-process element production?

Satellites' orbits vs. SF histories

~ evidence for environmental effects ~

Miyoshi & Chiba 2020

Fraction of stars formed after SF peak

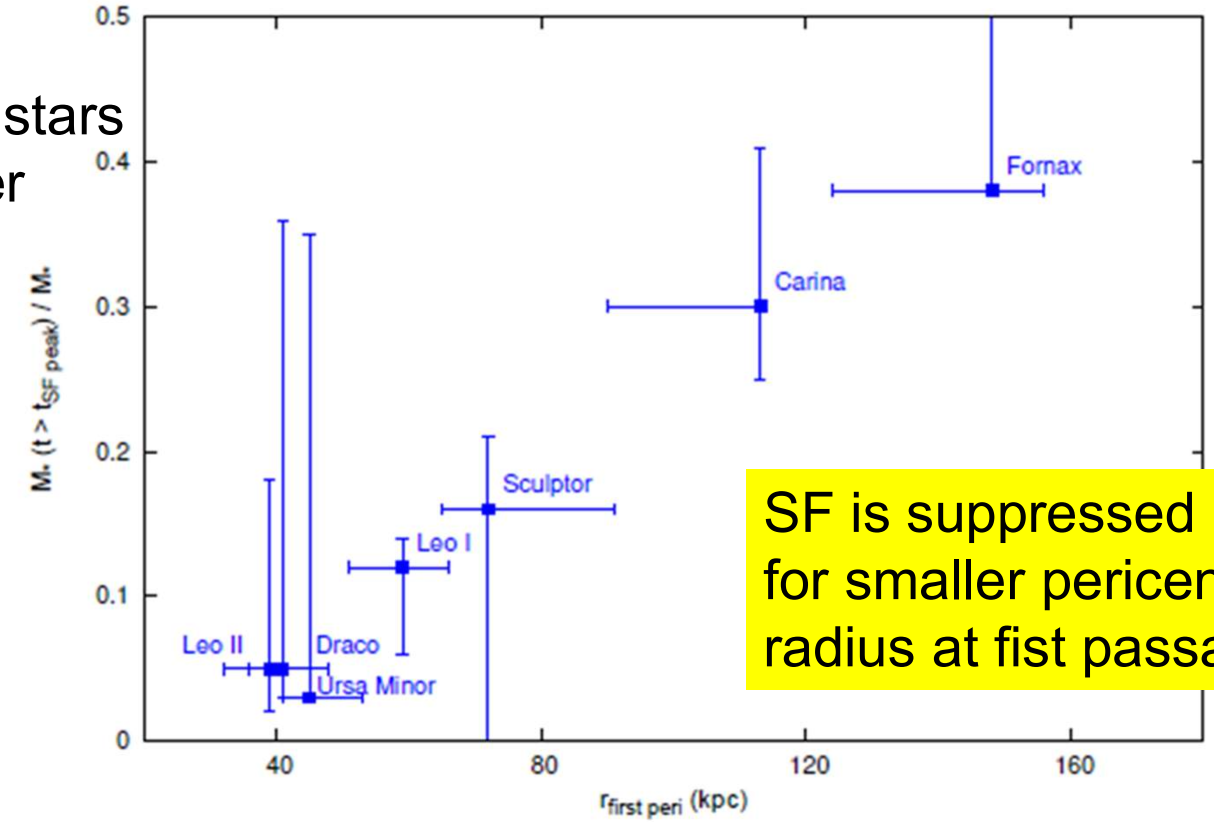

SF is suppressed more for smaller pericentric radius at fist passage

Pericenter at first passage (kpc)

Metallicity vs. luminosity relation

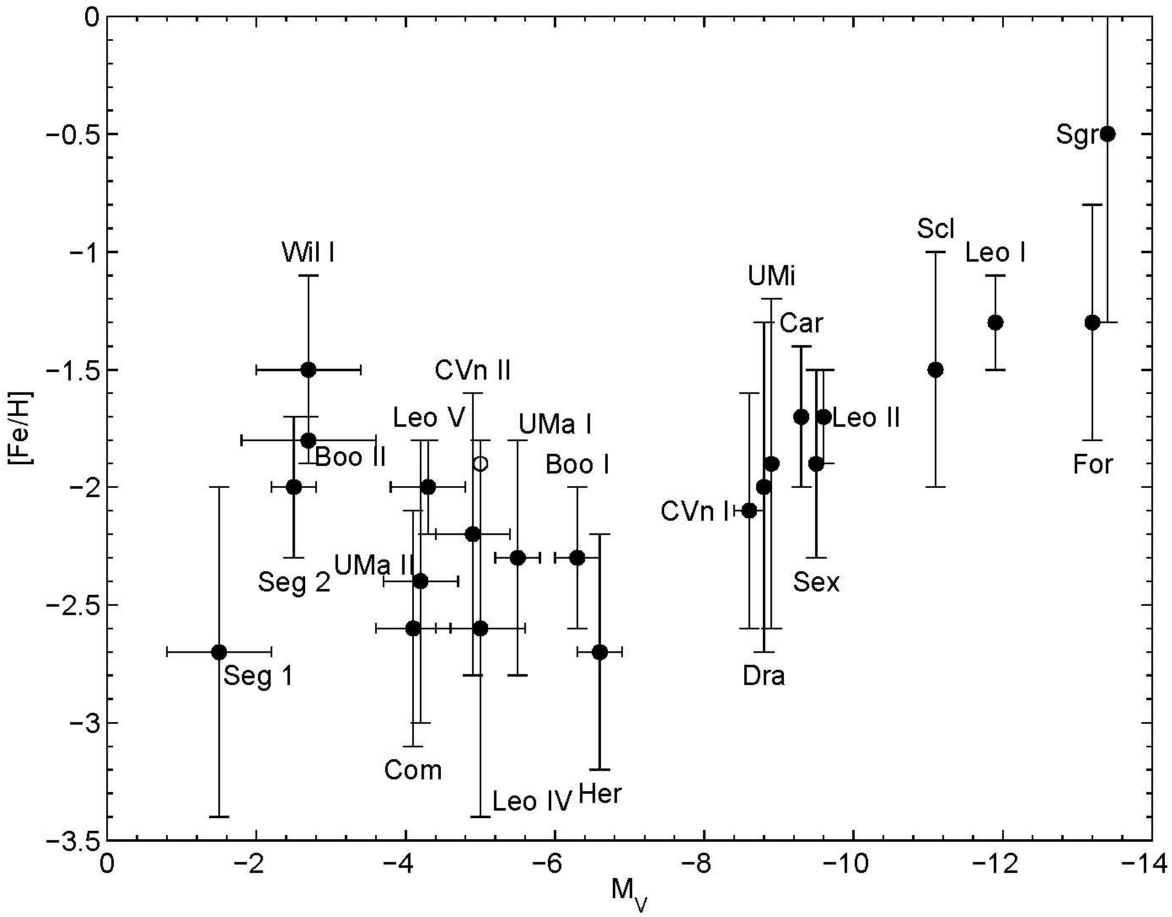

UFDs appear to show different metallicities

[α/Fe] ratios in several classical dSphs
(Tolstoy+ 2009)

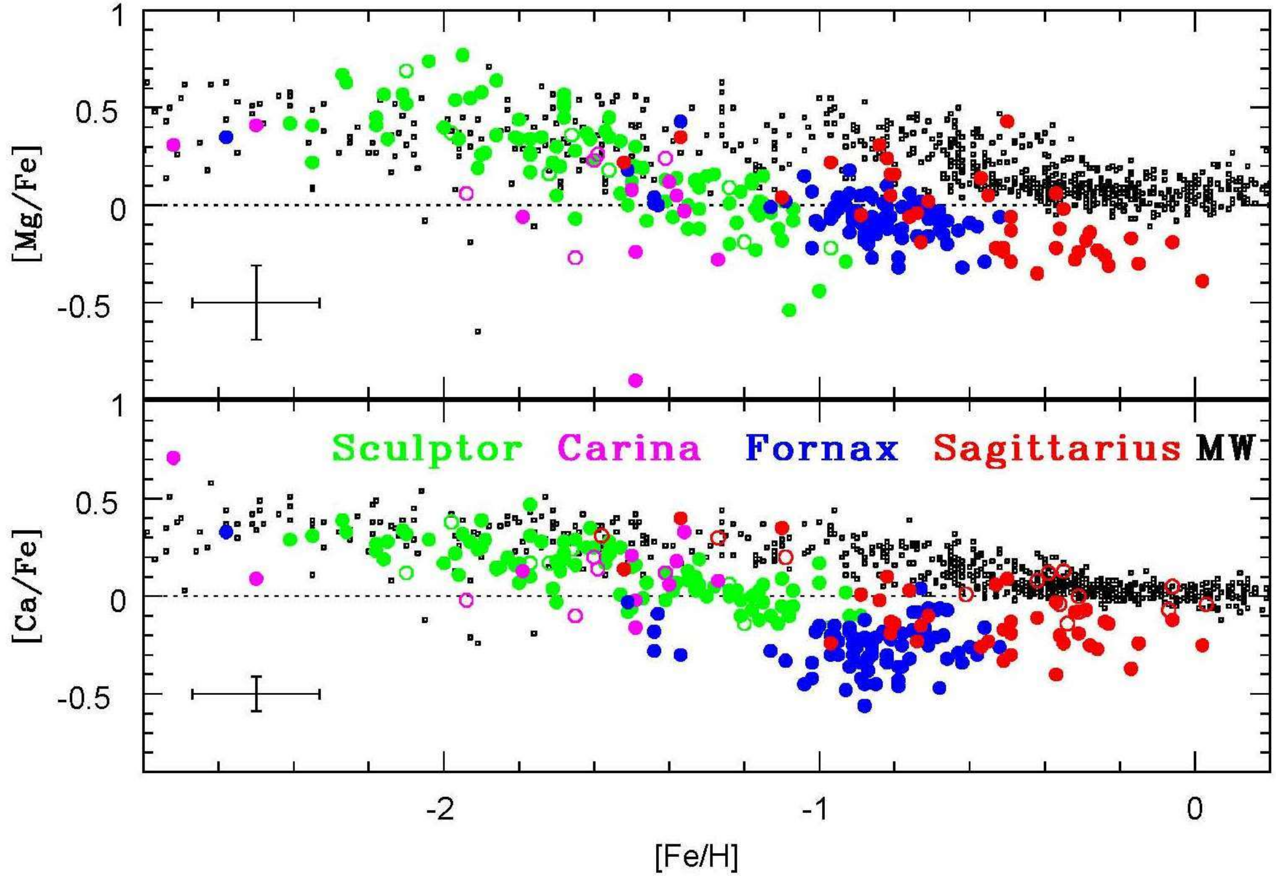

List of known UFD galaxies

名前	M_V [mag]	$D_\odot$ [kpc]	r_h [pc]	L_V [$L_\odot$]	$\langle$[Fe/H]$\rangle$ [dex]
CVn I	-8.6	218	564	2.3×10^5	-2.08
Her	-6.6	132	330	3.6×10^4	-2.58
Boo I	-6.3	66	242	3.0×10^4	-2.55
UMa I	-5.5	97	318	1.4×10^4	-2.29
Leo IV	-5.0	160	116	8.7×10^3	-2.58
CVn II	-4.9	160	74	7.9×10^3	-2.19
UMa II	-4.2	30	140	4.0×10^3	-2.44
Com	-4.1	44	77	3.7×10^3	-2.53
Boo II	-2.7	42	51	1.0×10^3	-1.79
Wil 1	-2.7	38	25	1.0×10^3	-2.19
Seg 2	-2.5	35	34	900	-2.26
Seg 1	-1.5	23	29	335	-2.72

HST results by Brown+2012
UFDs are very old systems (as old as M92)

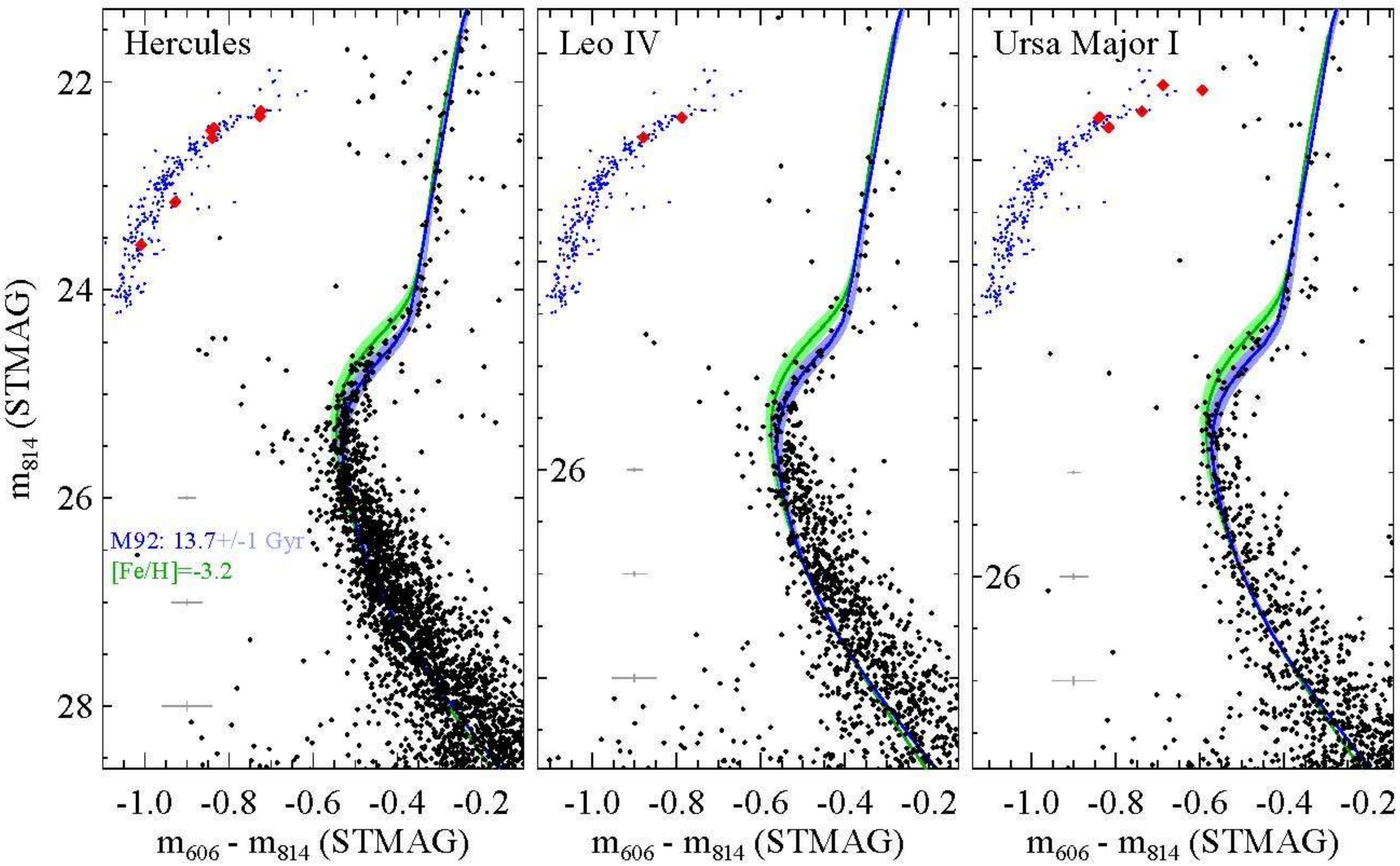

Synchronization of SF truncation within ~1 Gyr ?

Kirby+ 08

Assembly of the stars in ultra-faint dwarf galaxies reproduces the MW halo

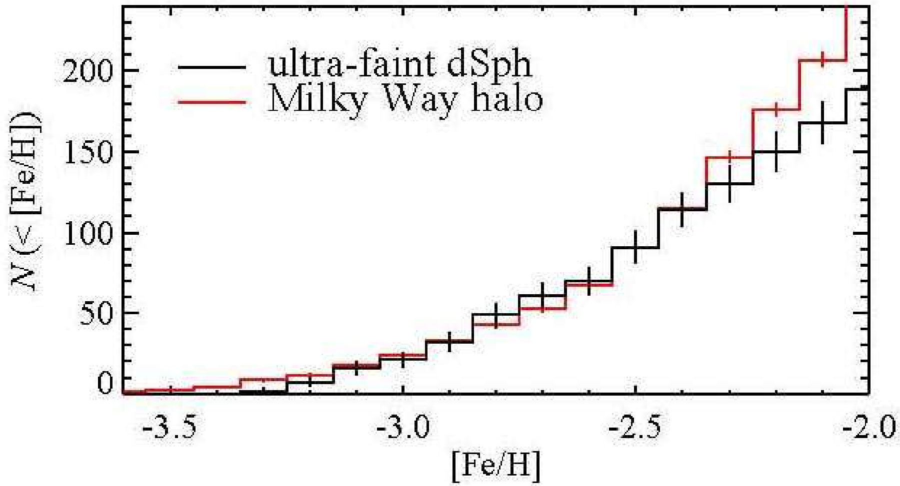

Tolstoy +08

UFDs show similar abundance pattern to the metal-poor MW halo

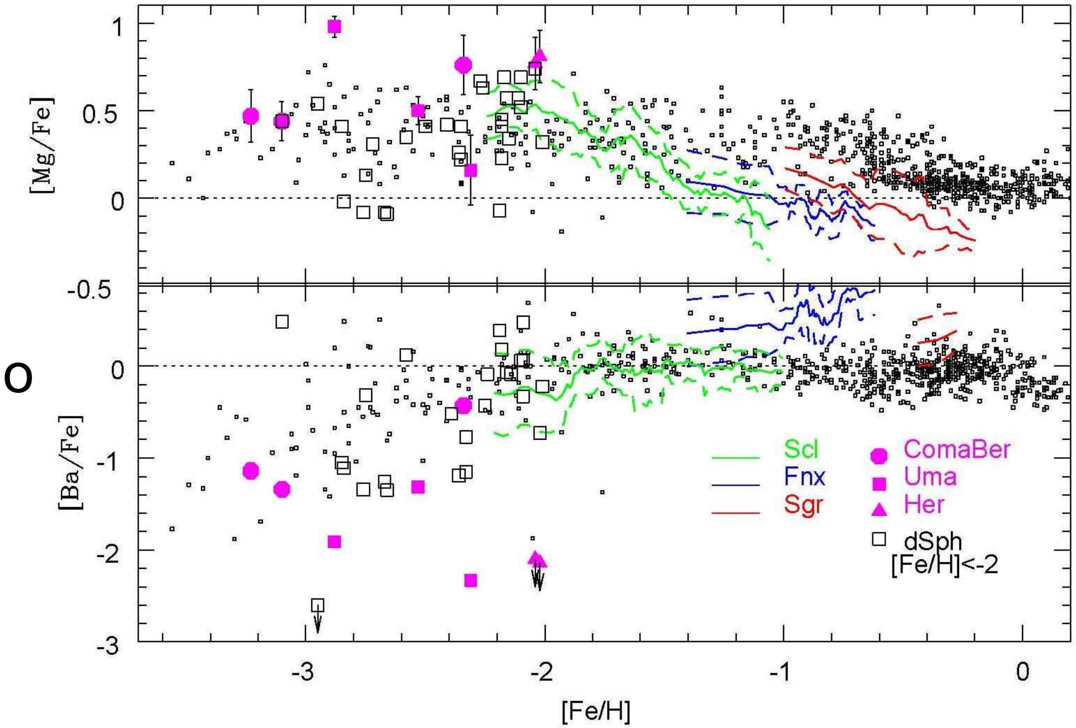

R-process enrichment in UFDs

Reticulum II: Ji et al. (2016)

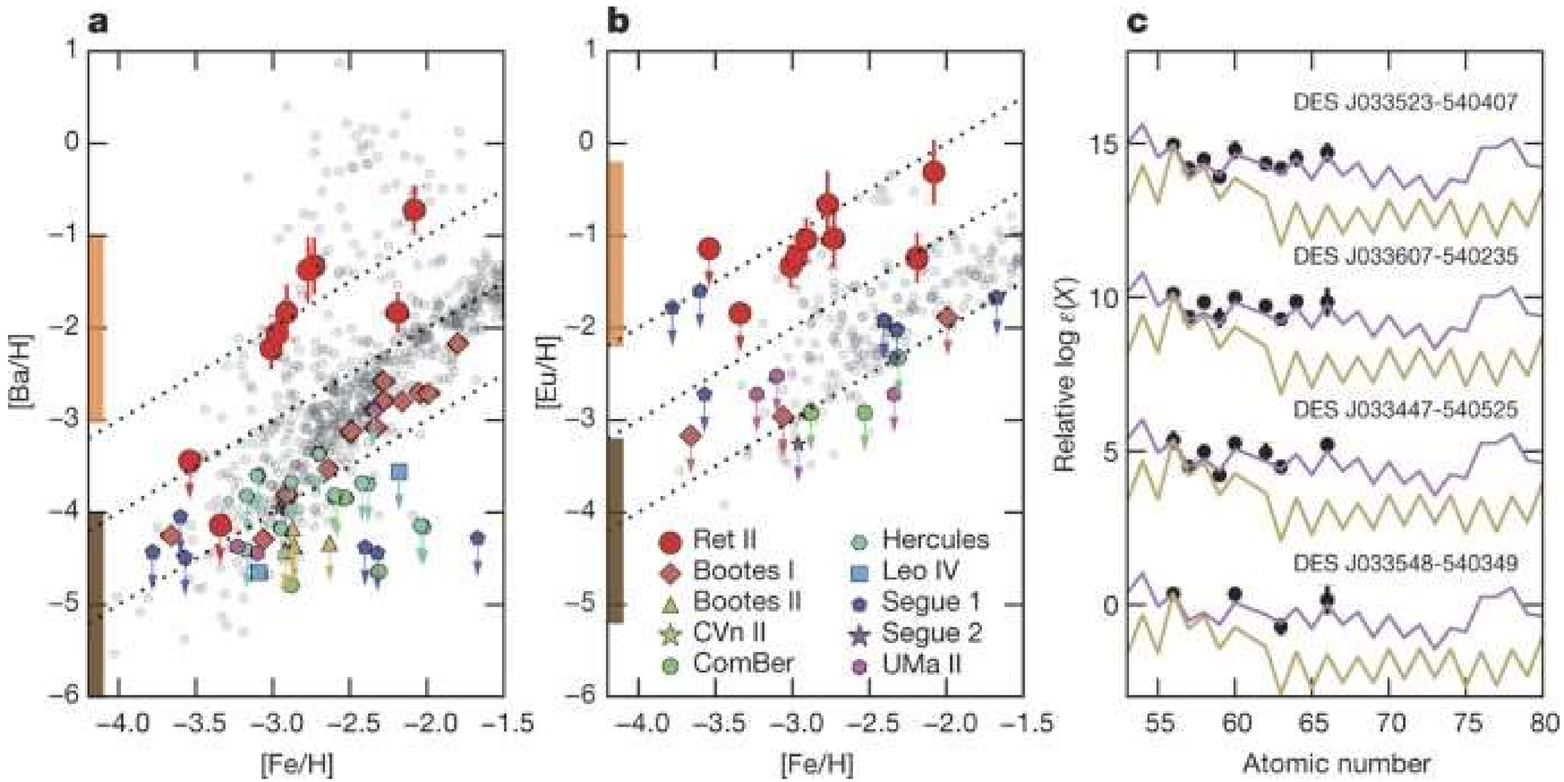

Solar r-process
Solar s-process

An event of NS mergers is suggested.

NS mergers and chemical evolution

Wanajo, Hirai, Prantzos (2021)
Chemical evolution of halo building blocks

Delay time distribution

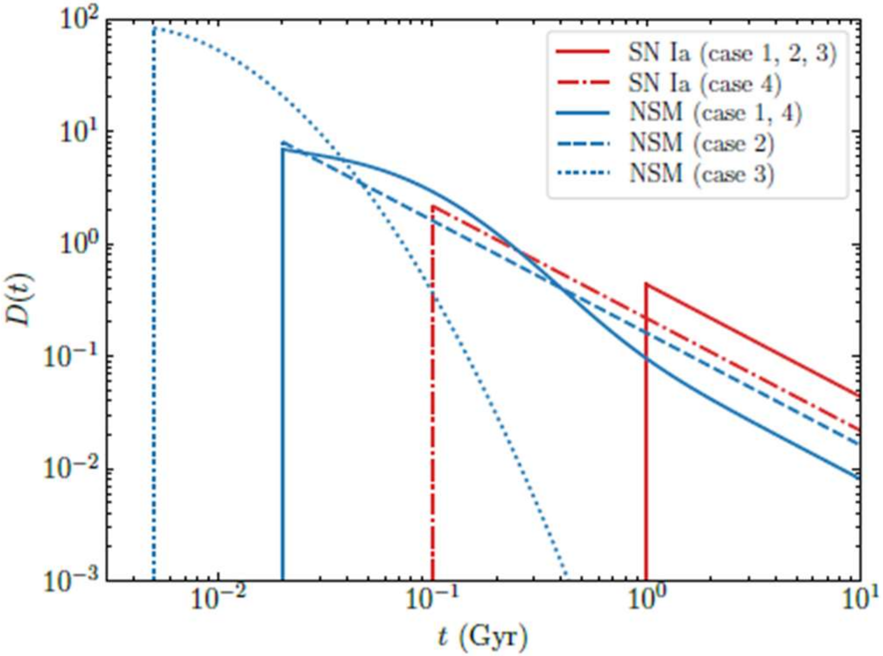

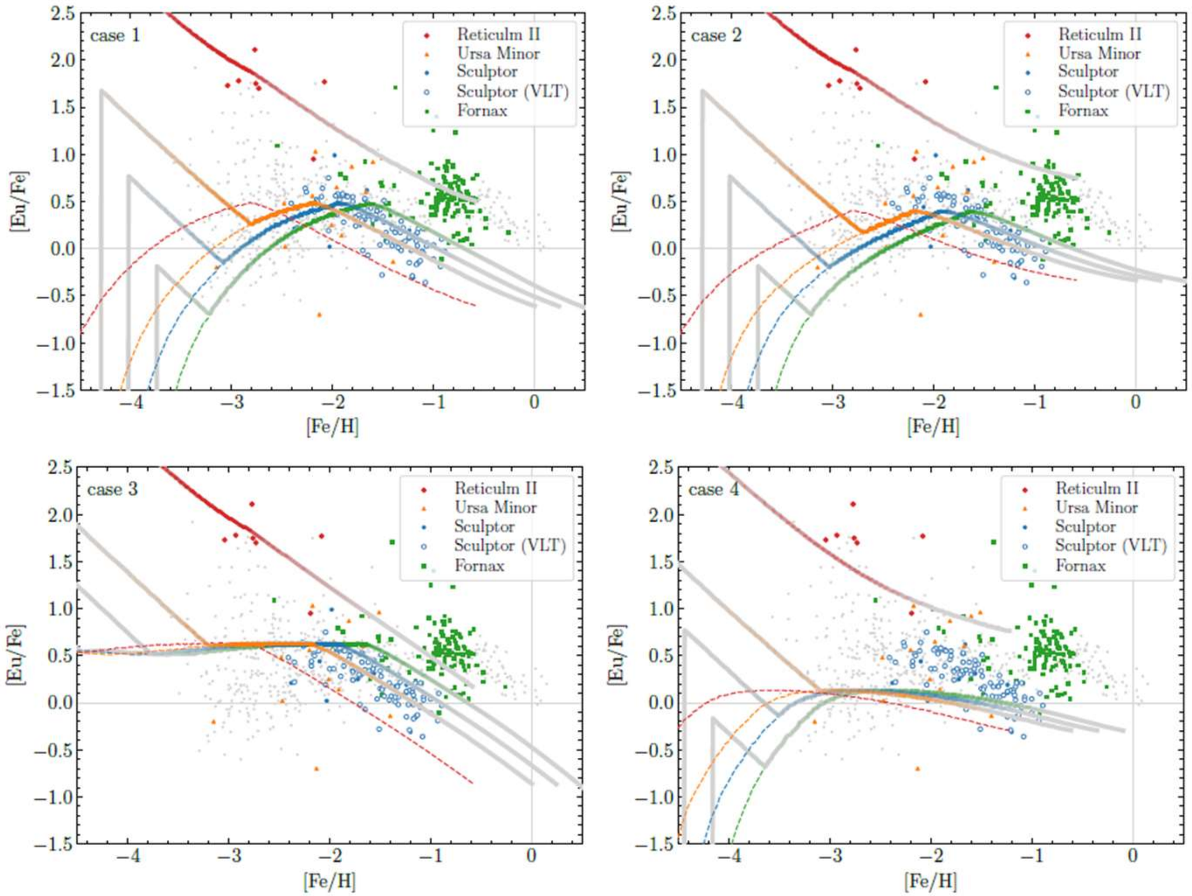

Cosmological zoom-in simulation for galaxy formation and origin of r-process enhanced stars

Hirai, Bees, Chiba, et al. (2022)

UFD galaxy as a site of r-process enrichment

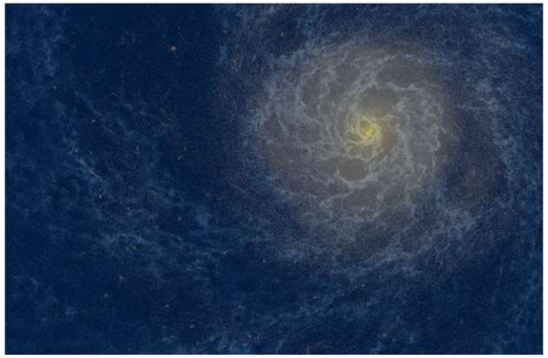

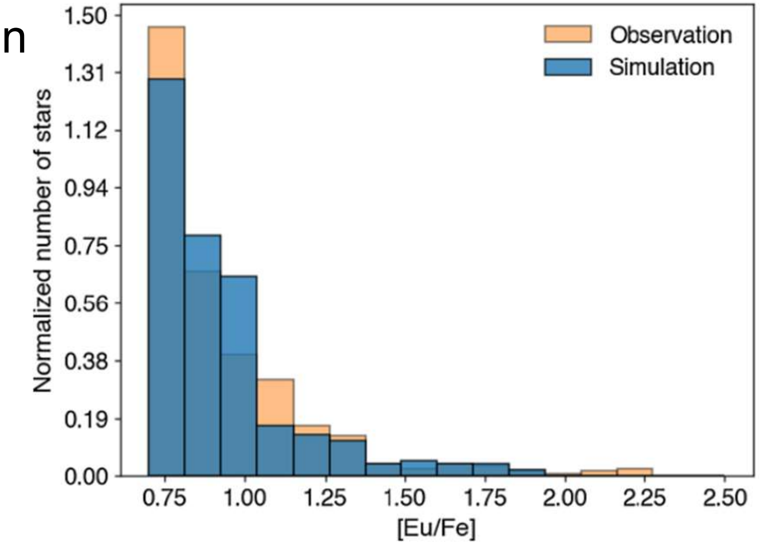

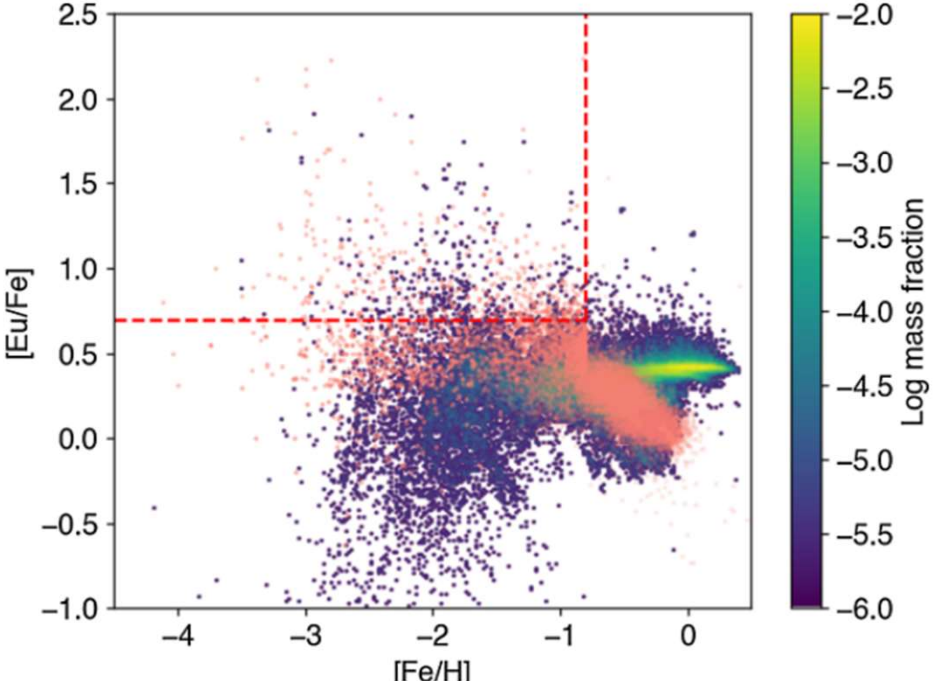

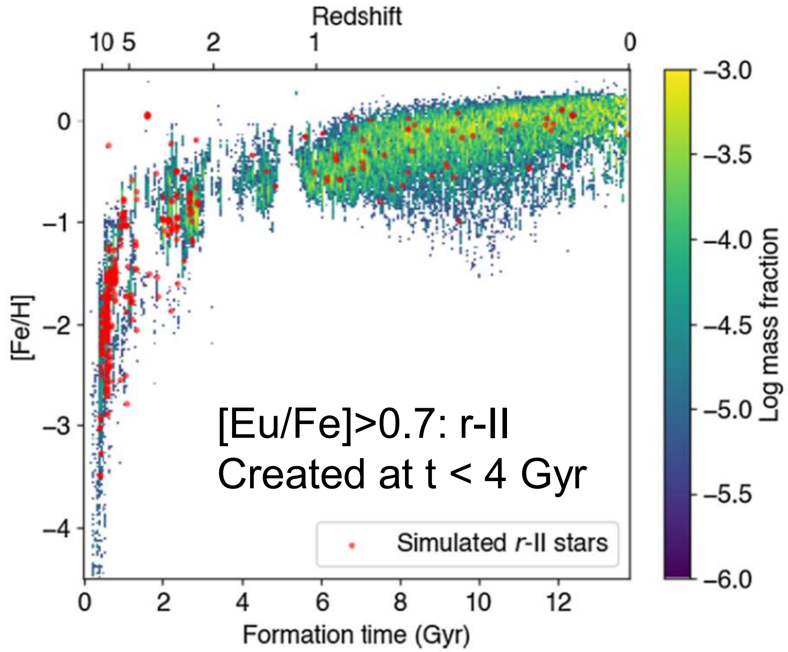

[Eu/Fe]>0.7: r-II
Created at t < 4 Gyr

6.4 Formation of the Andromeda galaxy

Andromeda Halo

(Ferguson et al. 2002)

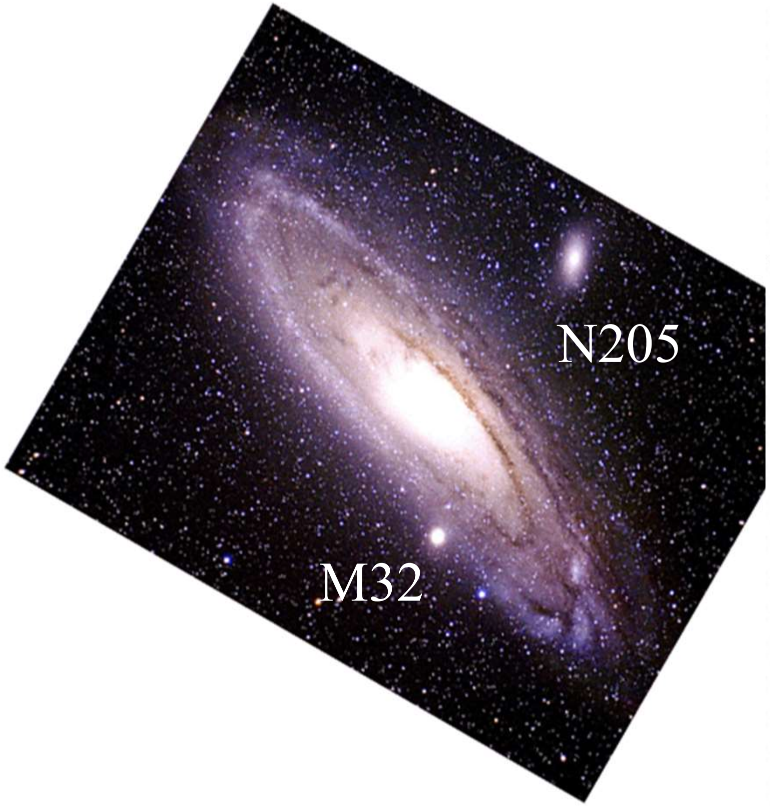

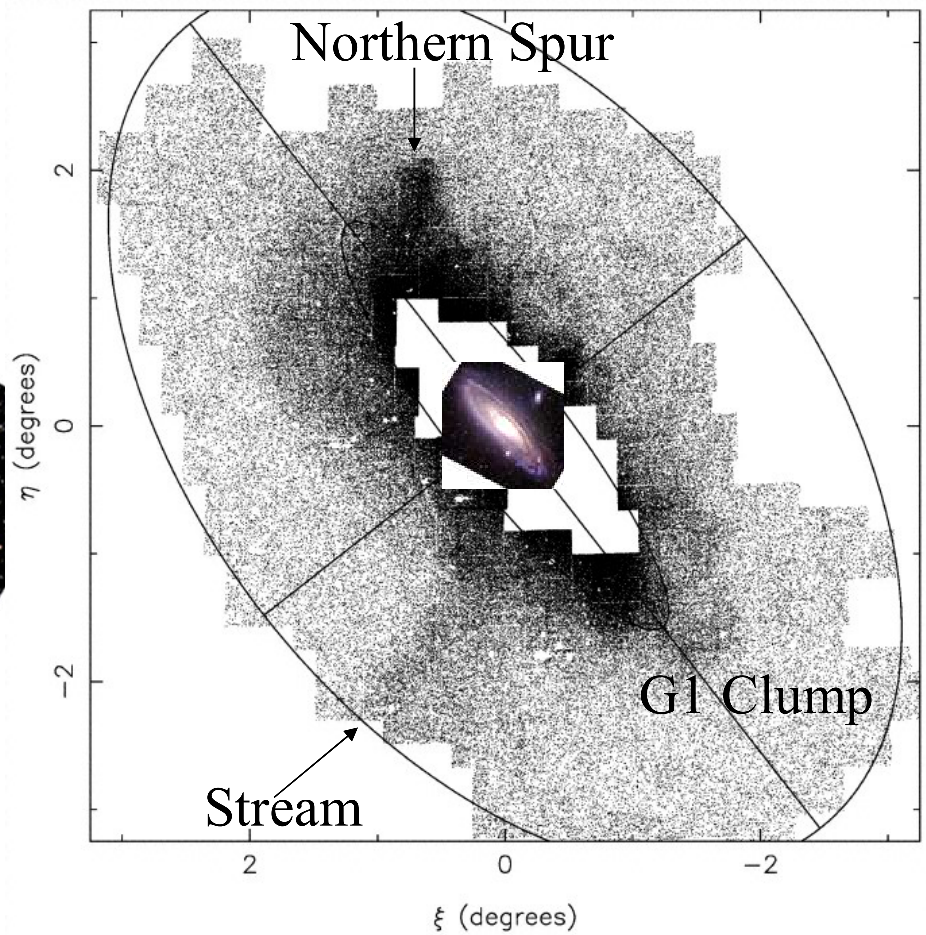

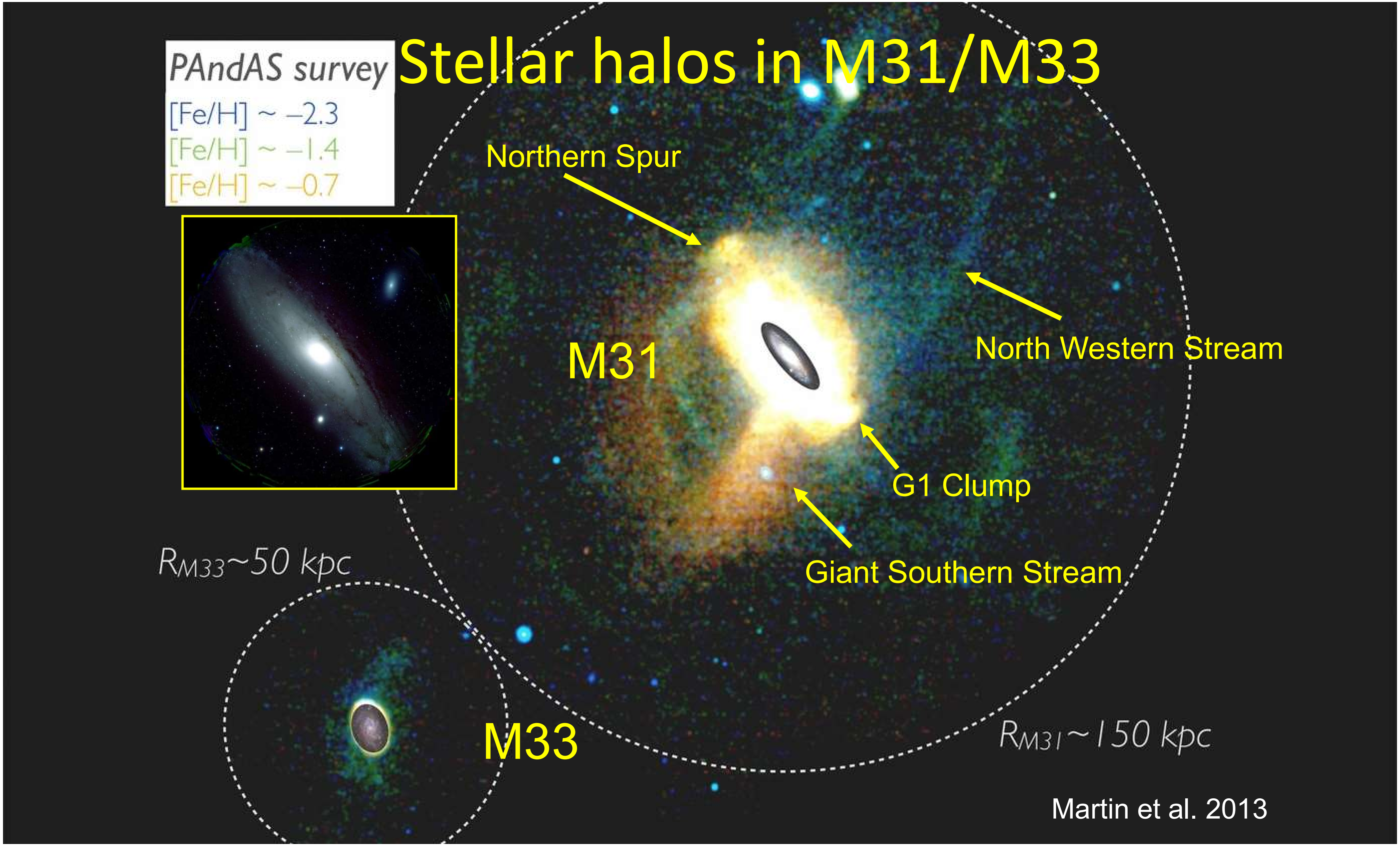
Stellar halos in M31/M33
PAndAS survey
[Fe/H] ~ –2.3
[Fe/H] ~ –1.4
[Fe/H] ~ –0.7
Northern Spur
M31
North Western Stream
G1 Clump
Giant Southern Stream
RM33~50 kpc
M33
RM31~150 kpc
Martin et al. 2013

Structure of the M31 halo

(Tanaka, Chiba et al. 2010)

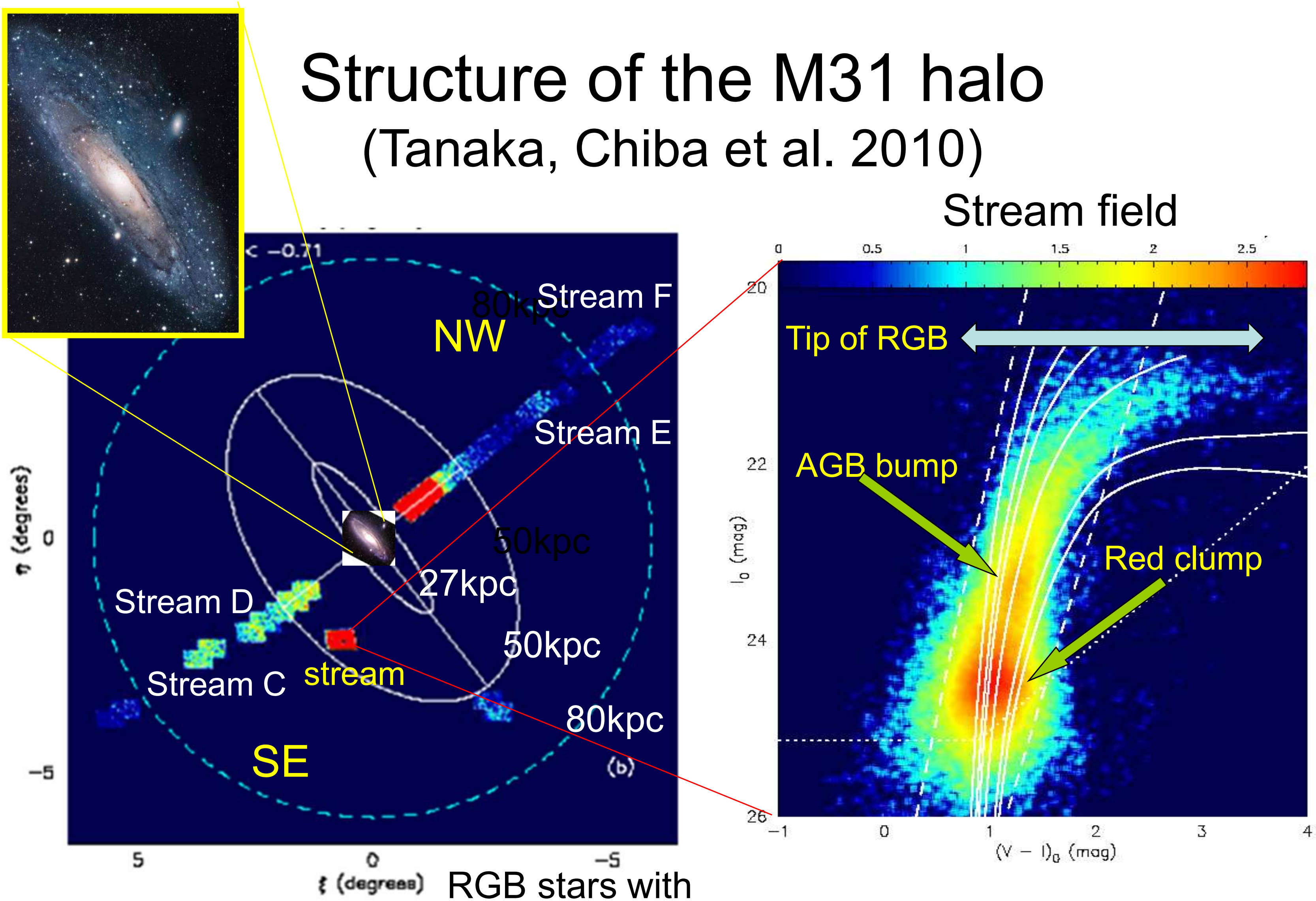

RGB stars with

I_0<24, V_0<24.8

-1.71<[Fe/H]<-0.71

(Photometric) metallicity distribution of Giant Southern Stream

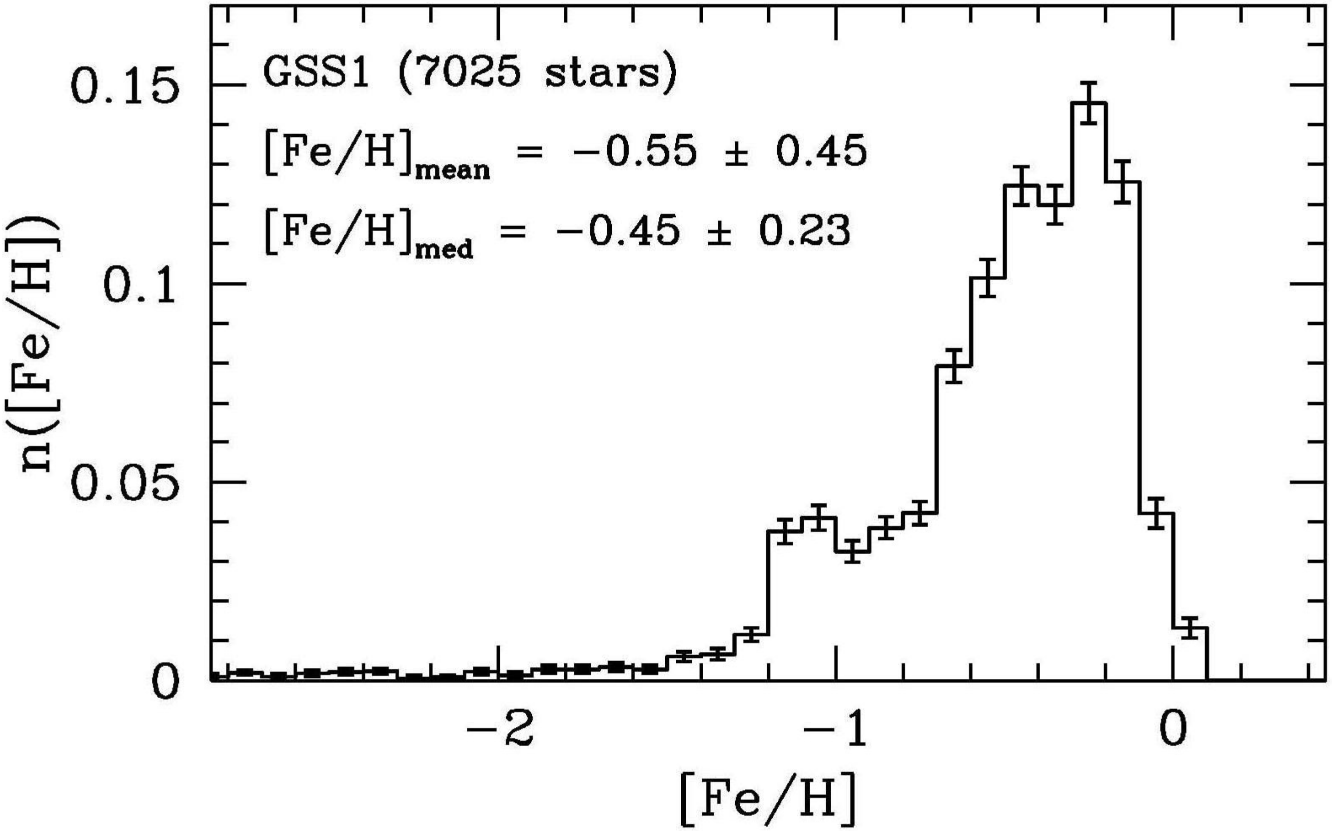

Numerical simulation of GSS

Hotta, Mori, Otaki, & Kirihara in prep

Progenitor: disk galaxy
with metallicity gradient

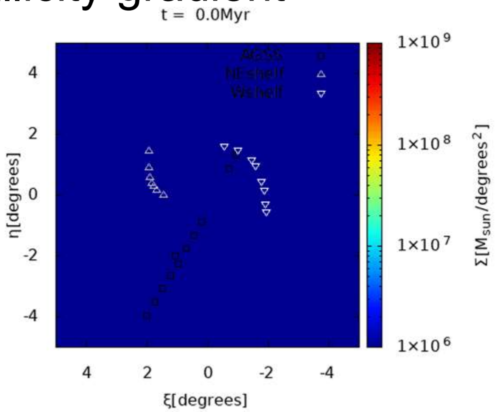

Metal-poor($[Fe/H] < -1.0$) Rich($[Fe/H] > -1.0$)

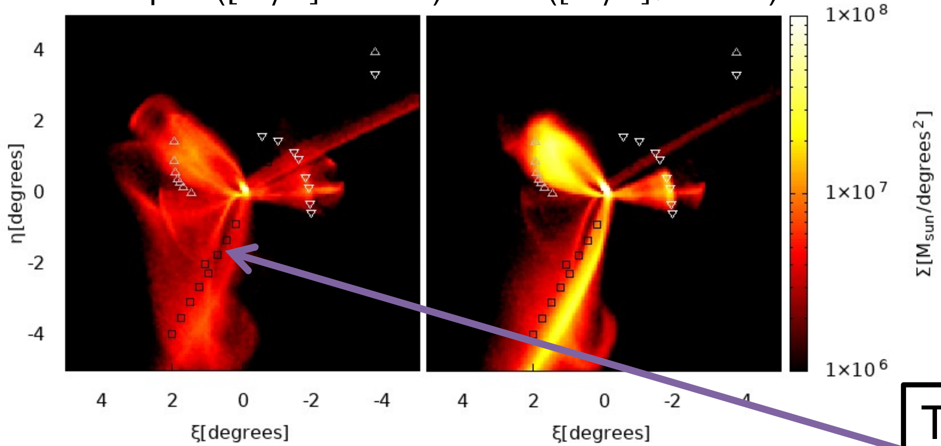

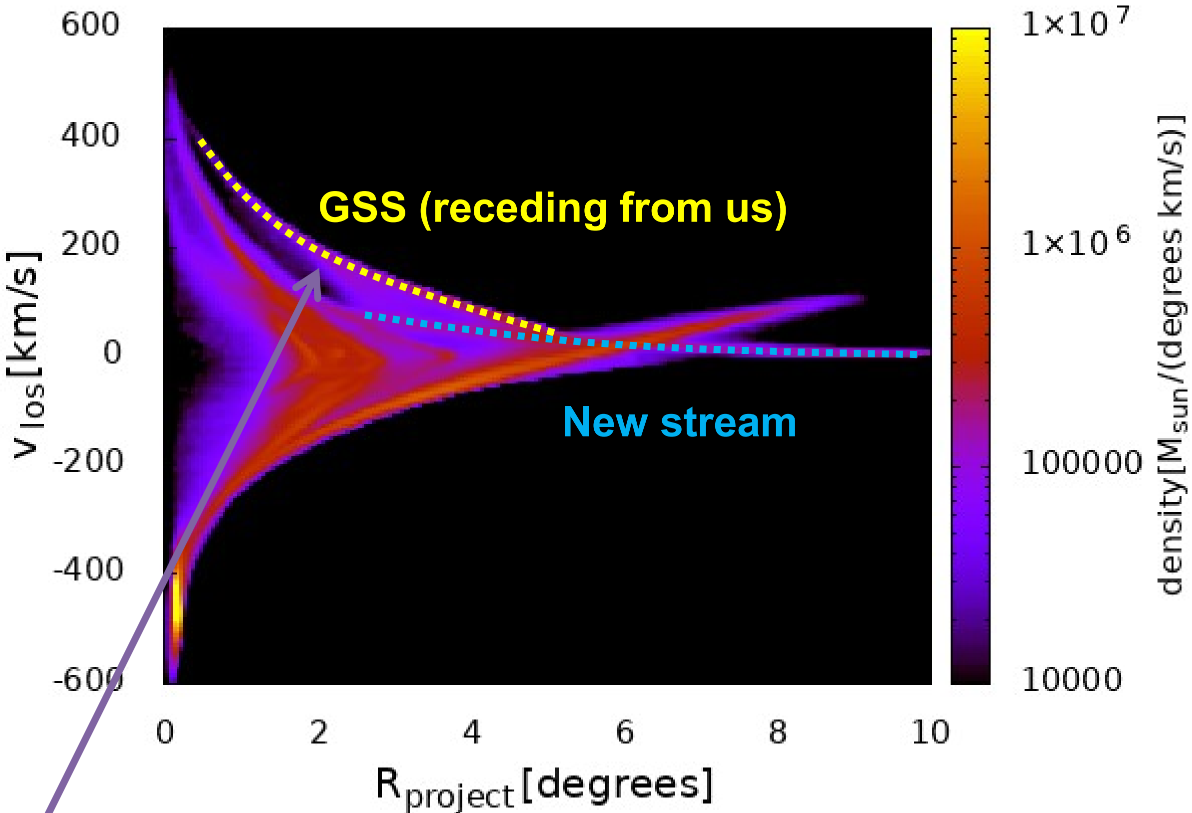

This **metal poor, faint, and positive velocity stream** at the eastern side of GSS is **missing in DESI map**.

Dey et al. (2023) with DESI
Machine-learning selection of
very red, metal-rich, bright RGBs
2 < (g-i) < 4, z < 21.5 mag

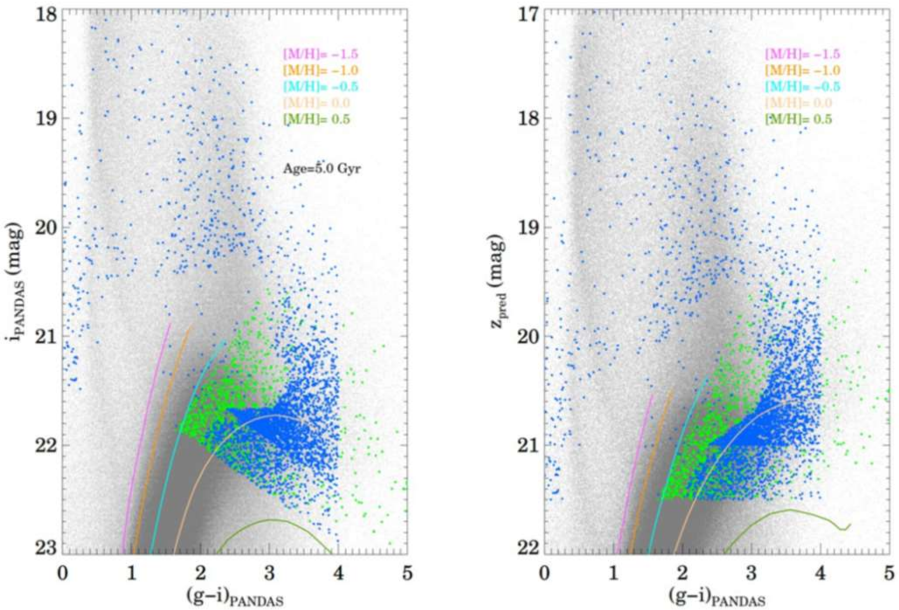

Complicated selection function
Biased for very metal-rich stars
(-0.5 < [Fe/H] < +0.5)

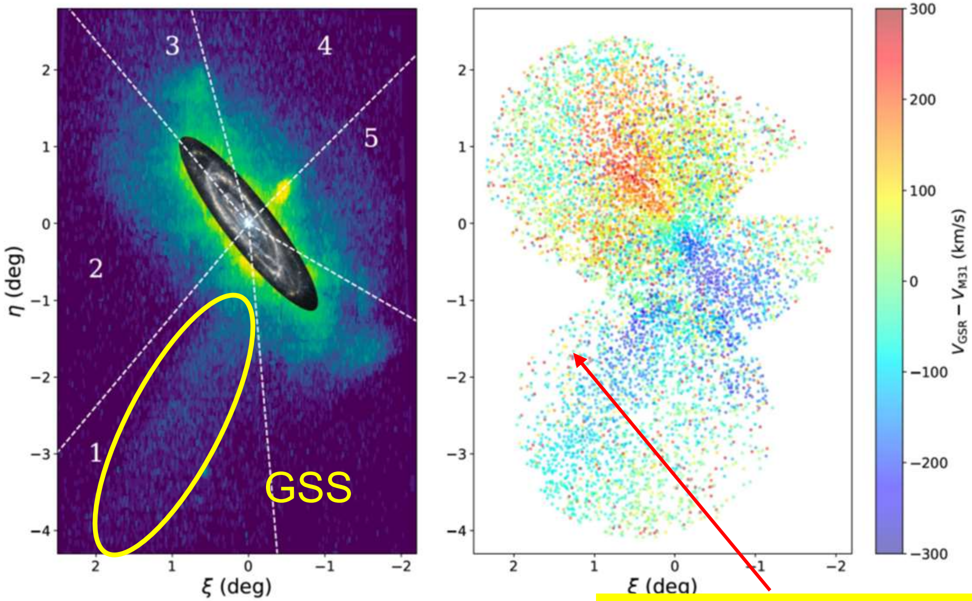

Los velocities (wrt. M31)

Metal-poor substructures are entirely disappeared!

Phase-space diagram

Los velocities (wrt. M31)

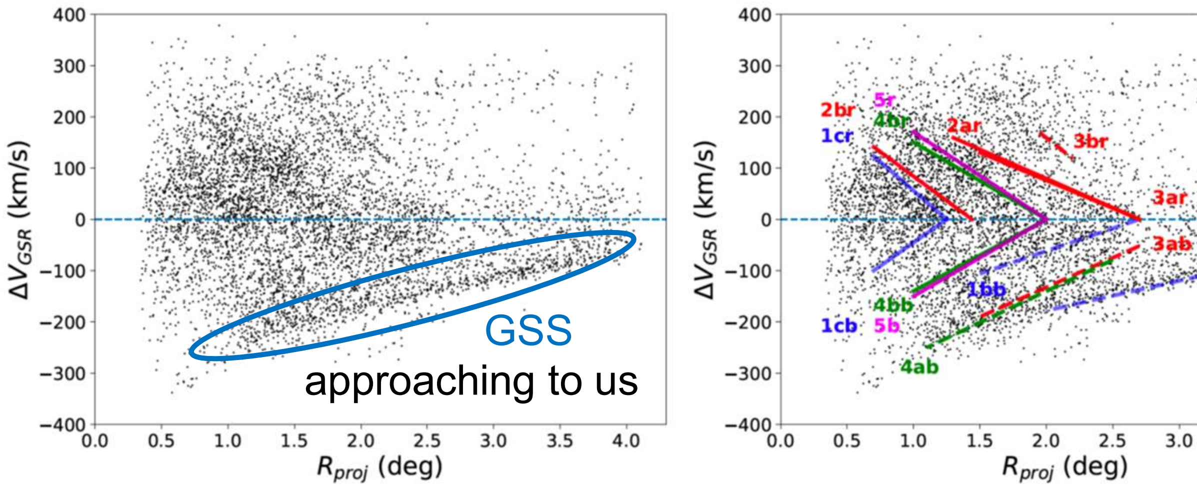

Important features in CM diagram

- RGB bump (RGBb)
  - Evolutionary pause when the H-burning shell crosses a discontinuity left by the convective envelope
- Tip of RGB (TRGB)
  - He-burning ignition through the He flash
  - Nearly constant I-band mag ⇒ standard candle
  - 843±48kpc, 855±48kpc > D=770kpc
- Red Clump (RC)
  - Clustered feature of red HB (He core-burning) stars being metal-rich / young age
- AGB bump (AGBb)
  - Clustered feature of AGB stars at the beginning of He shell-burning evolution

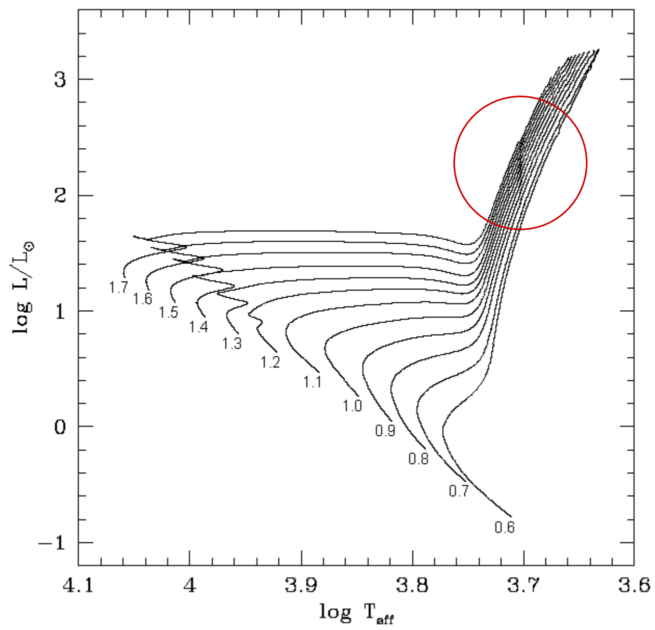

Luminosities of RGBb, RC, & AGBb depend on age.
⇒ age distribution

Alves & Sarajedini 1999

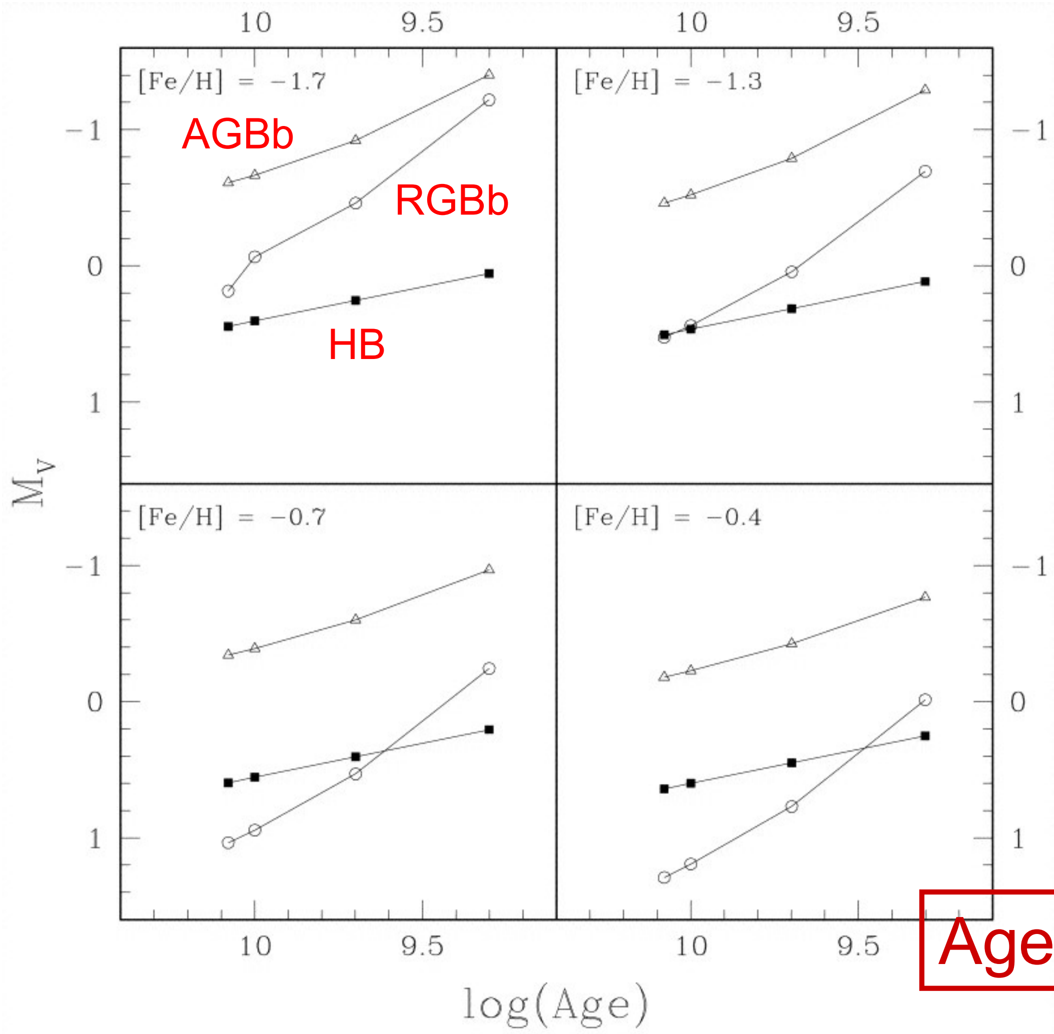

Fainter
for
Z↑M↓

Age indicator

Age calibration for giant stream

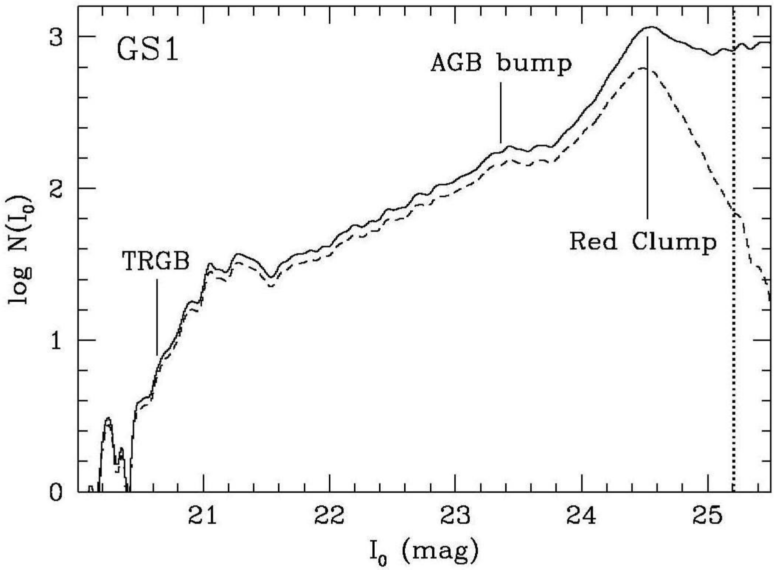

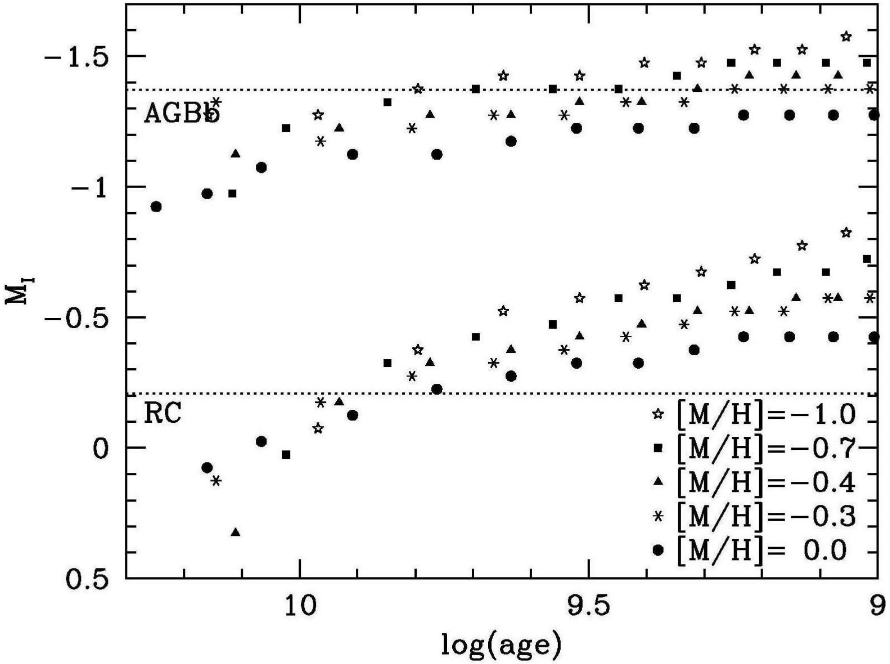

Mean Age ～ 7.1 Gyr

Tanaka+2010

North Western Stream

Komiyama, Chiba et al.2018

North Western Stream

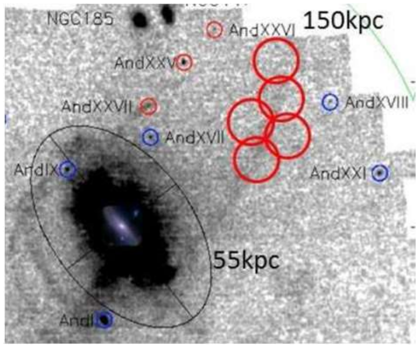

Subaru/HSC data

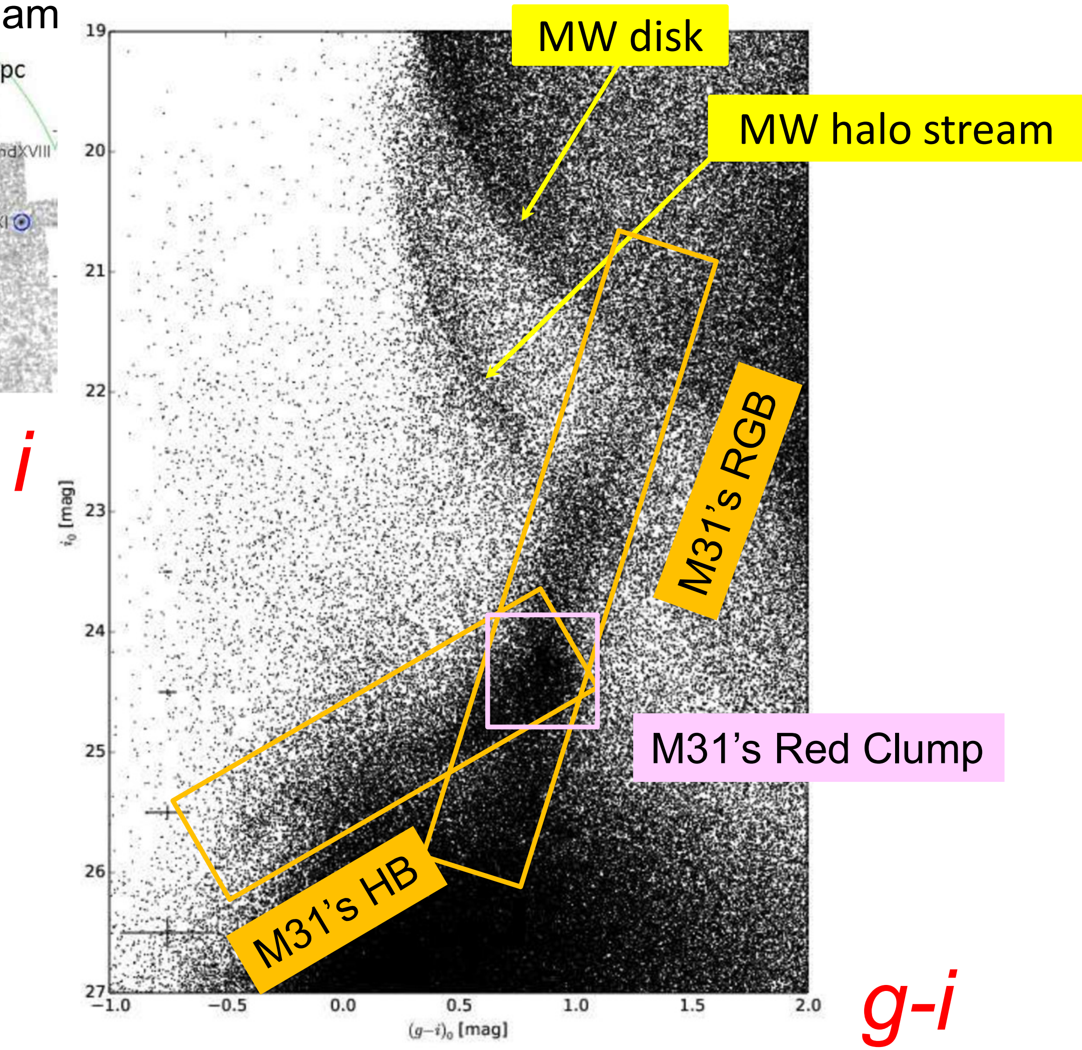

Komiyama et sl.2018

North Western Stream

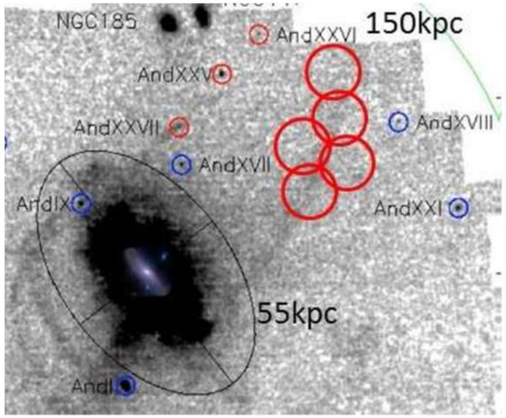

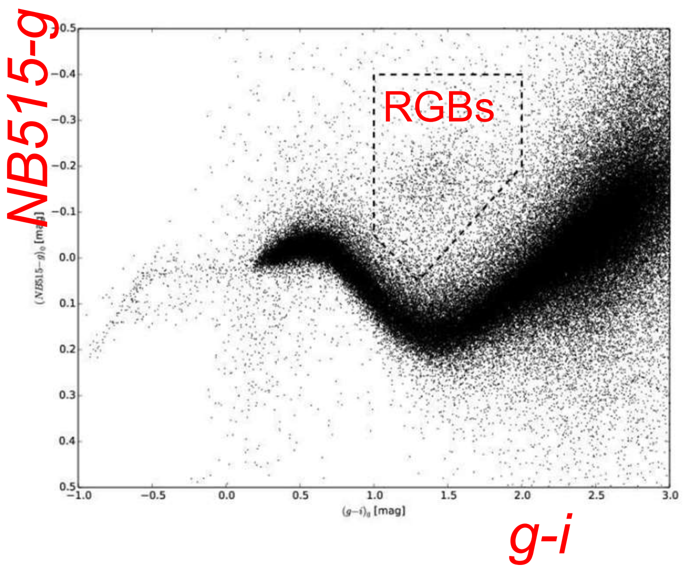

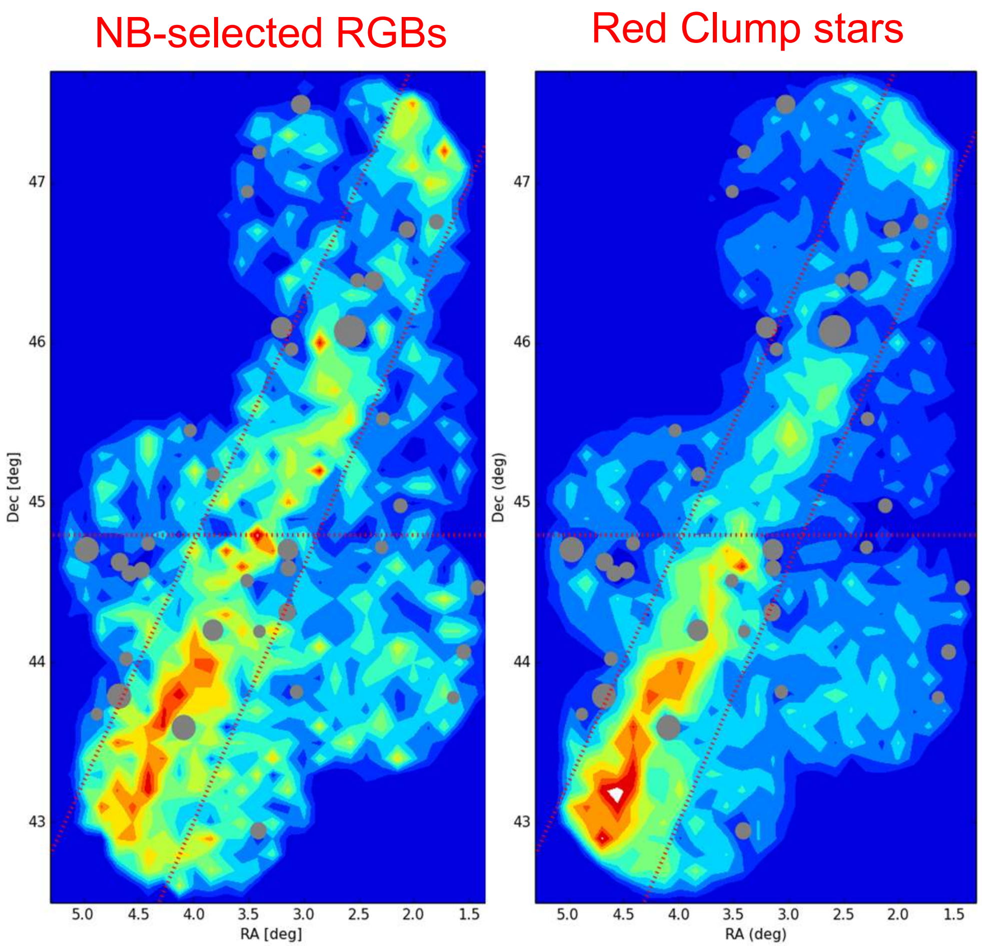

Formation of the NW stream

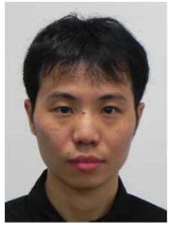

Yohei Miki
(U. Tokyo)

- Progenitor of the NW stream
  - Satellite with $M = 5 \times 10^7 M_\odot, N = 2^{20}$
- Interaction with a subhalo
  - Mass: $M = 10^{9.5} M_\odot$
  - Test orbit: 2 circular orbits with $r = 145\ \mathrm{kpc}$, $v_{\mathrm{rot}} = 147\ \mathrm{km\ s^{-1}}$ (orbit 0, orbit 1)
- LOS velocity fields after 300 Myr
- Effect of a subhalo mass

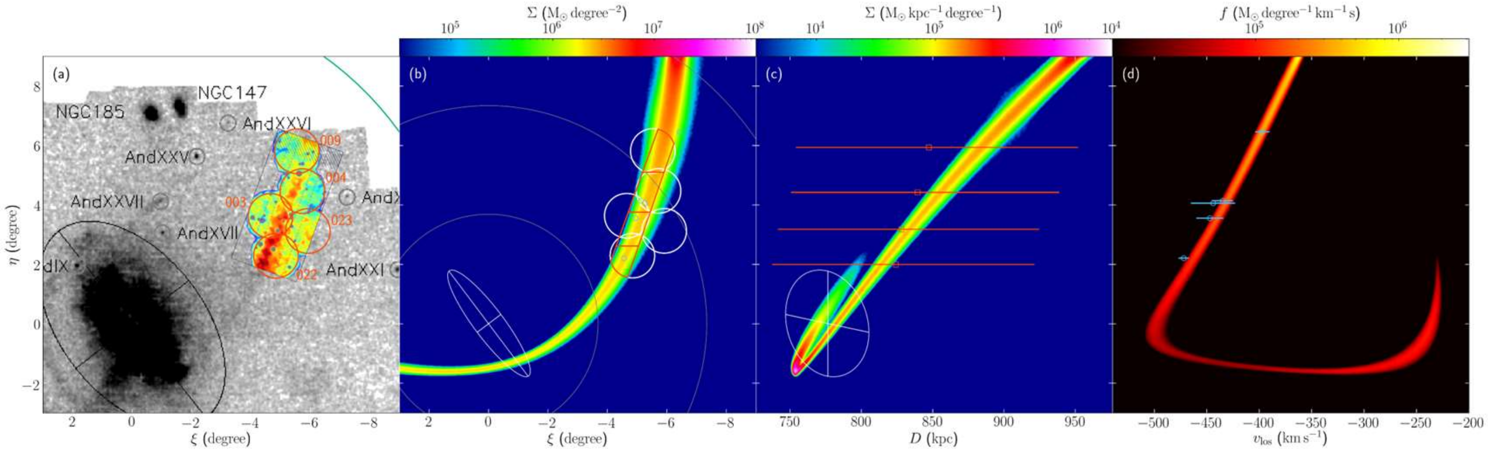
Σ (M⊙ degree^{-2})
Σ (M⊙ kpc^{-1} degree^{-1})
f (M⊙ degree^{-1} km^{-1} s)
(a)
(b)
(c)
(d)
NGC147
NGC185
AndXXVI
AndXXV
AndXXVII
AndXVII
AndXXI
dIX
009
004
003
023
022
η (degree)
ξ (degree)
D (kpc)
v_{los} (km s^{-1})

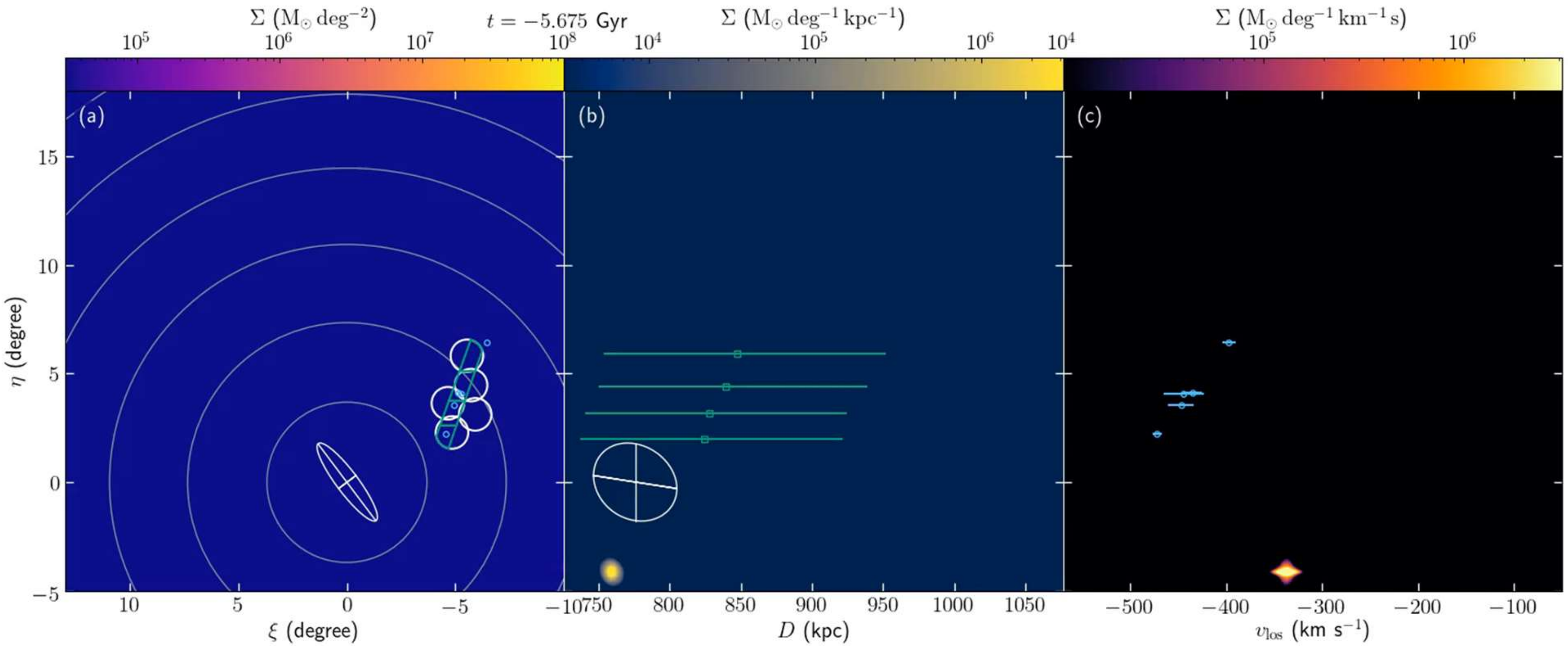
Σ (M⊙ deg^{-2})
t = −5.675 Gyr
Σ (M⊙ deg^{-1} kpc^{-1})
Σ (M⊙ deg^{-1} km^{-1} s)
(a)
(b)
(c)
η (degree)
ξ (degree)
D (kpc)
v_{los} (km s^{-1})

True size of Andromeda

M31（アンドロメダ銀河）
の真の大きさ

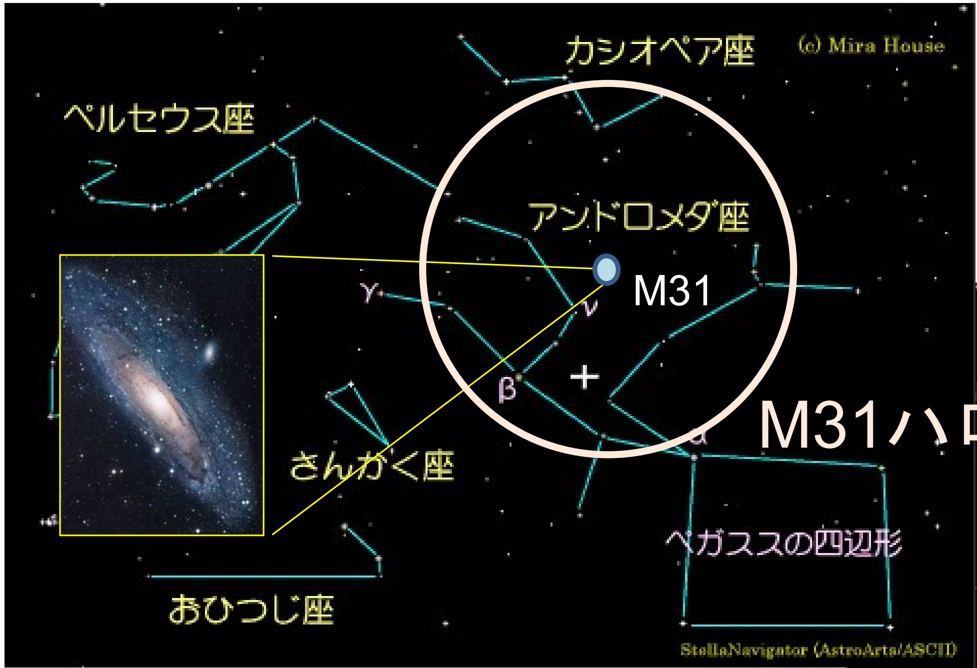

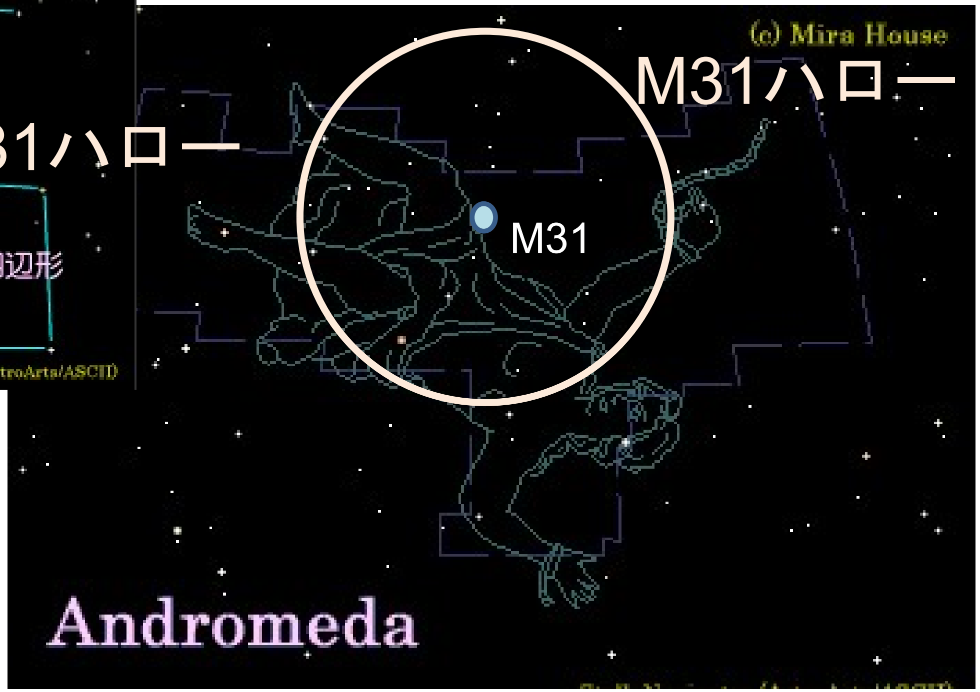

Future Prospects

Major telescopes/instruments

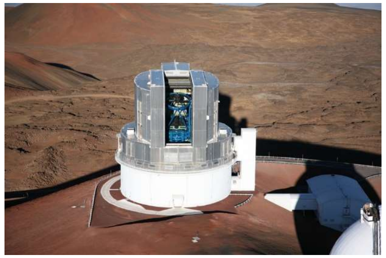

Subaru
HSC
PFS : 2024-
Ultimate:

ALMA

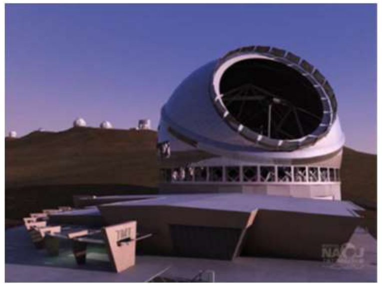

TMT
WFOS
HROS
NIRES
2028?

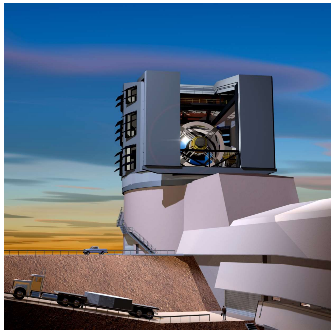

Vera C. Rubin (LSST)
2023-

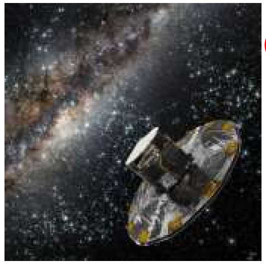

Gaia

JWST
NIRCam
NIRSpec
MIRI
2022-

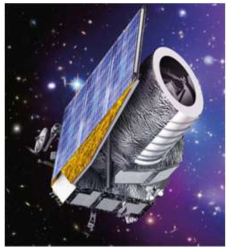

Euclid
YJH
2023-

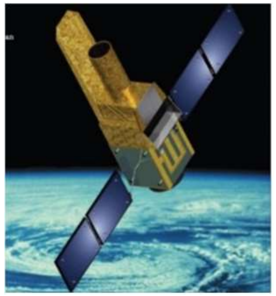

JASMINE
NIR astrometry
Late 2020

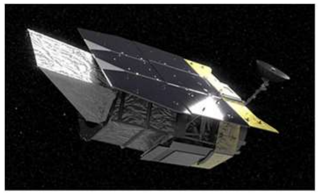

Nancy Grace Roman Space Telescope (WFIRST)
2026-

Subaru/PFS
(Prime Focus Spectrograph)

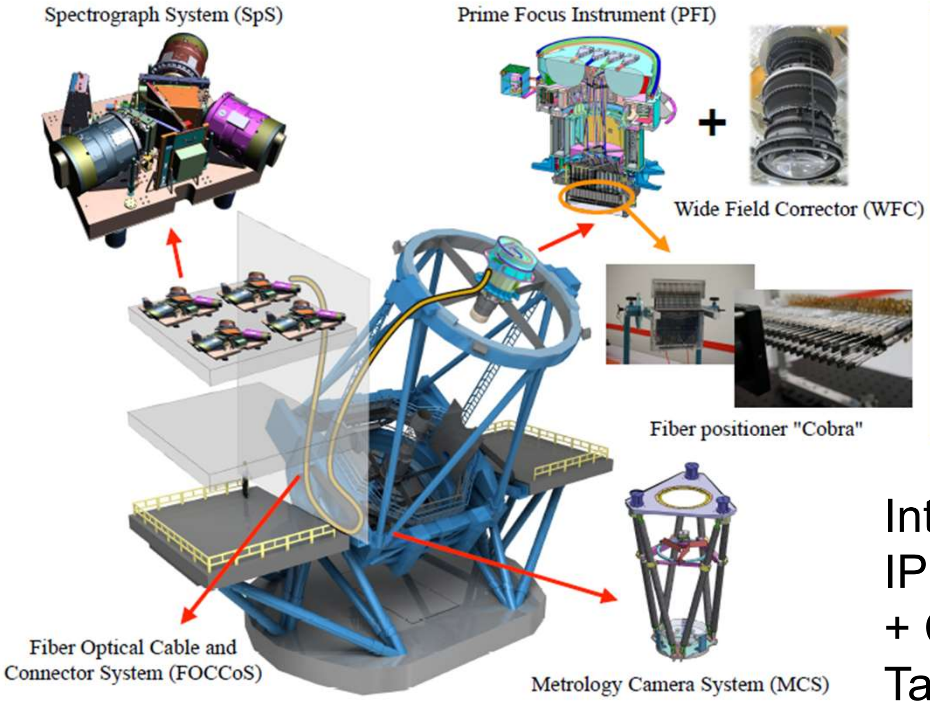

FOV: 1.3 deg in diameter
2400 fiber positioners
λ: 380~1,300 nm
(3 channels: Blue, Red, IR)
R: ~3,000 (LR), 5,000 (MR)
Scientific run: 2024 ~

International collaboration:
IPMU (U. of Tokyo) & NAOJ/Subaru
+ Caltech/JPL, Princeton, JHU, LAM,
Taiwan, UK, Brazil, China

Science in 3 main areas
- Cosmology, Distant Galaxies, Galactic Archaeology

TMT
(Thirty Meter Telescope)

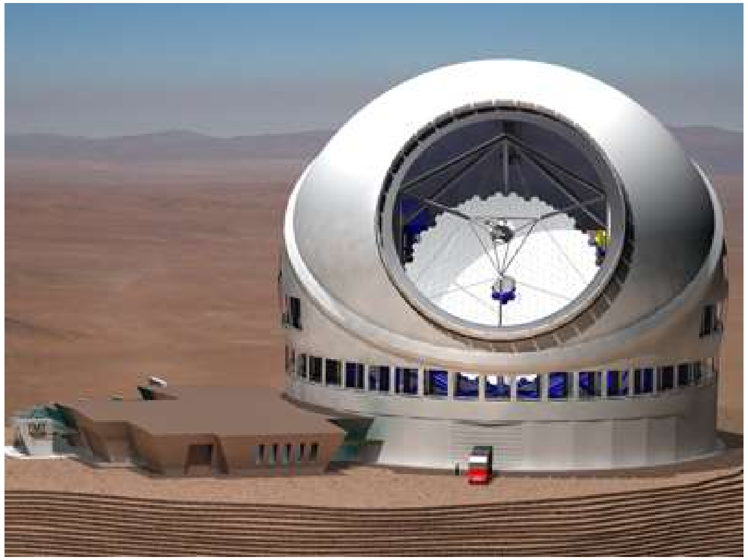

WFOS, IRIS, IRMS,
HROS, NIRES etc.
R~5,000 for m_V<26 mag
R~50,000 for m_V<21 mag
First light: 2028~?

Goal: ultimate understanding of galaxy formation
based on resolved stars in the local universe

M31/M33's halo survey with PFS

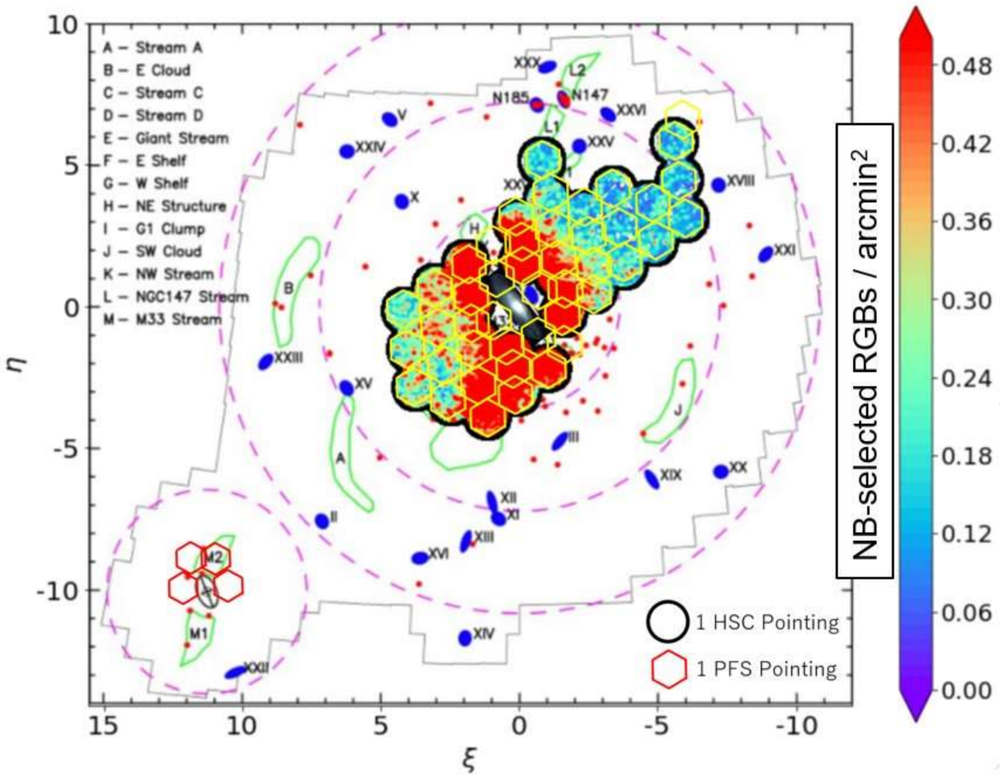

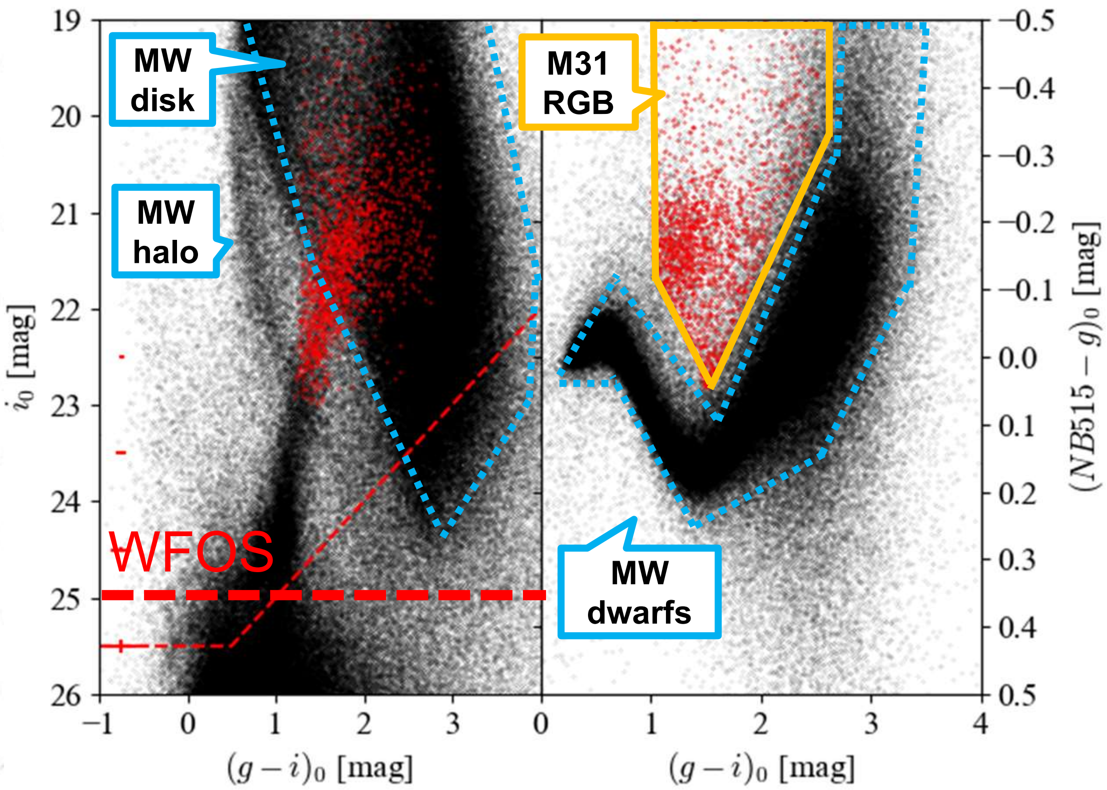

200～400 RGBs/field with PFS

TMT/WFOS

M31 has the [α/Fe] bimodality？

PNe: O/Ar ratio measurements (Arnaboldi et al. 2022)

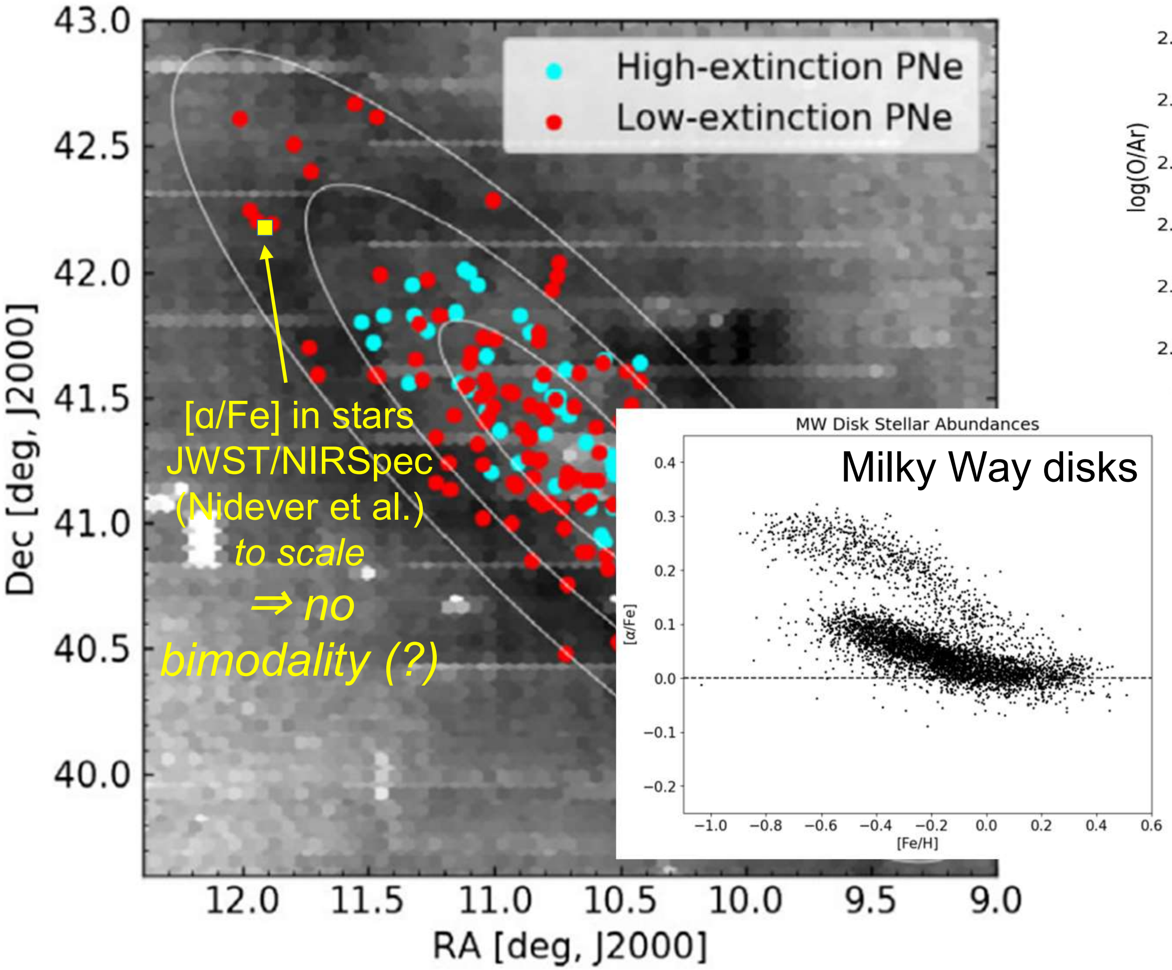

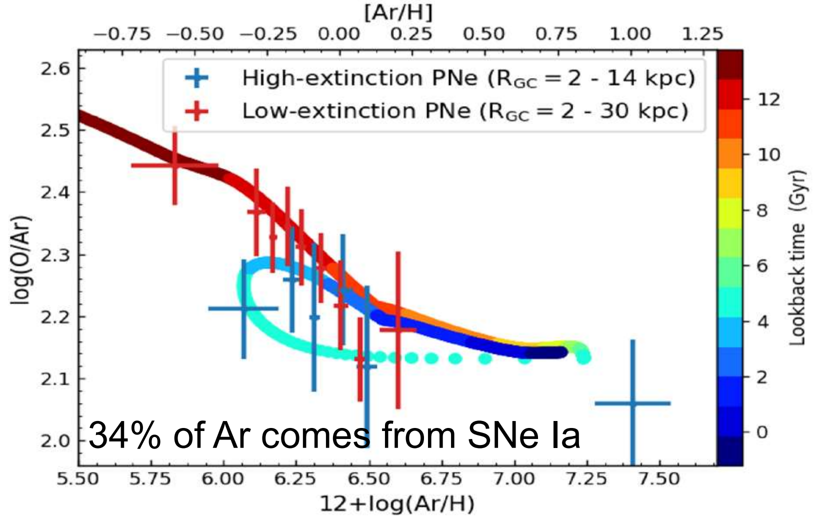

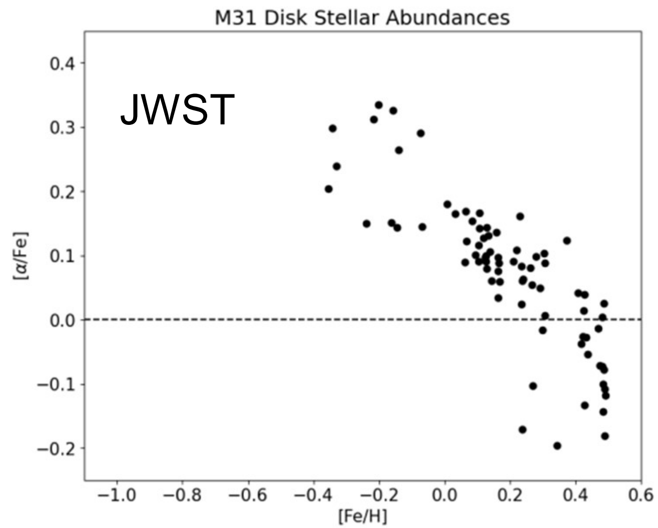

M31 has the [α/Fe] bimodality？

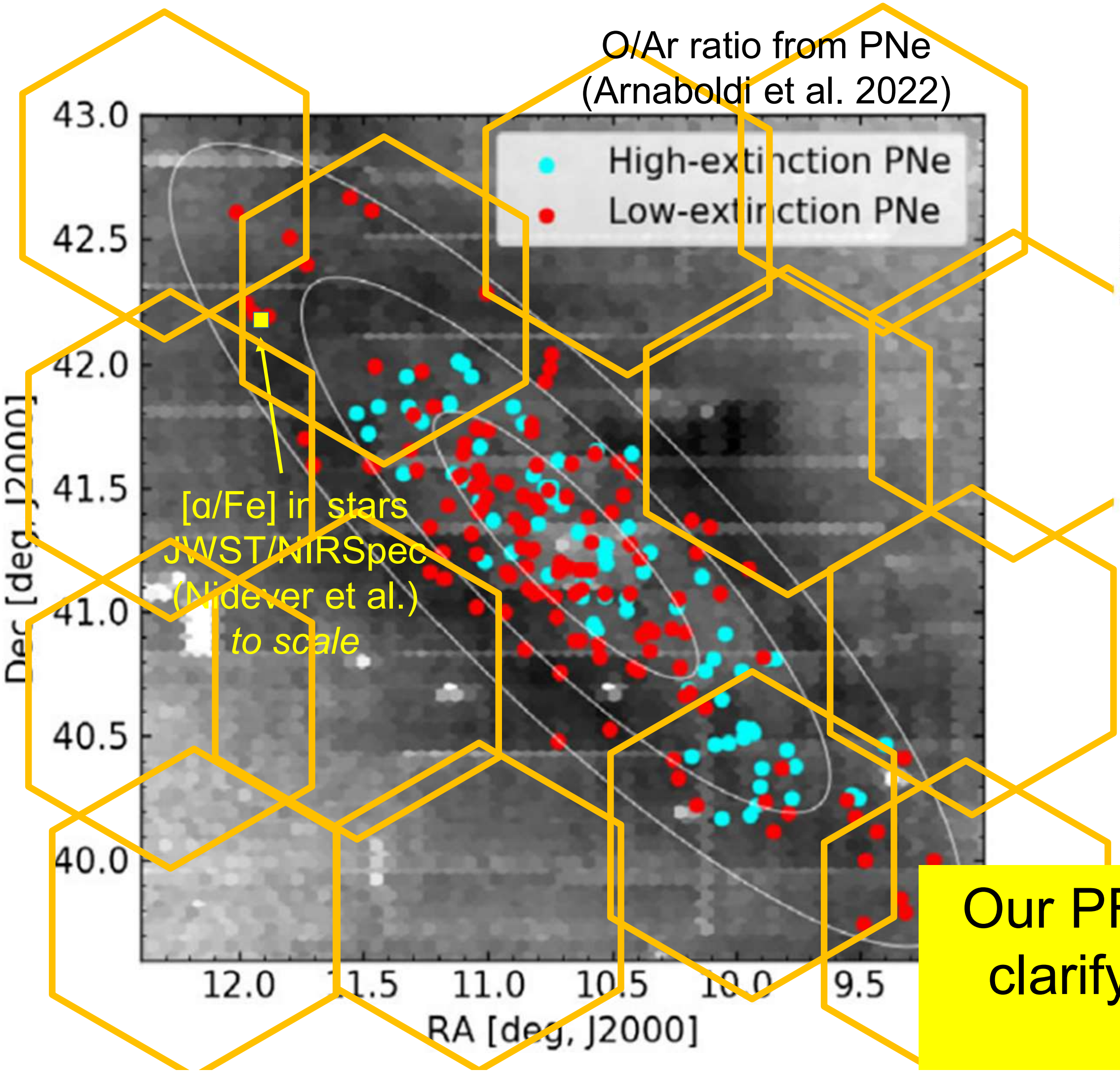

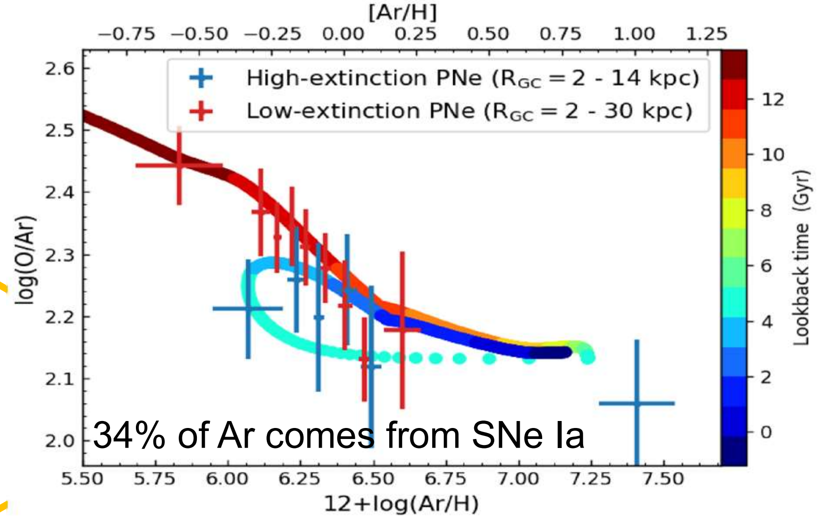

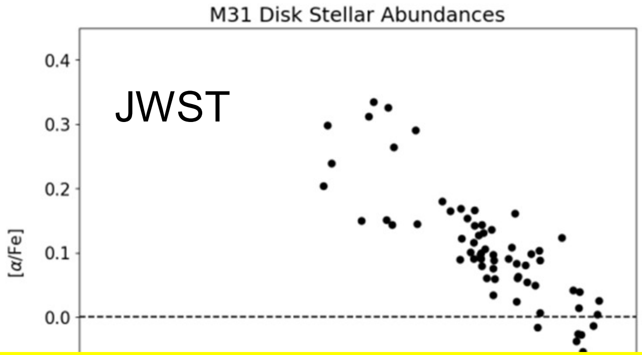

Our PFS survey will cover larger disk areas to clarify this bimodality for understanding disk formation process

Nearby group of galaxies

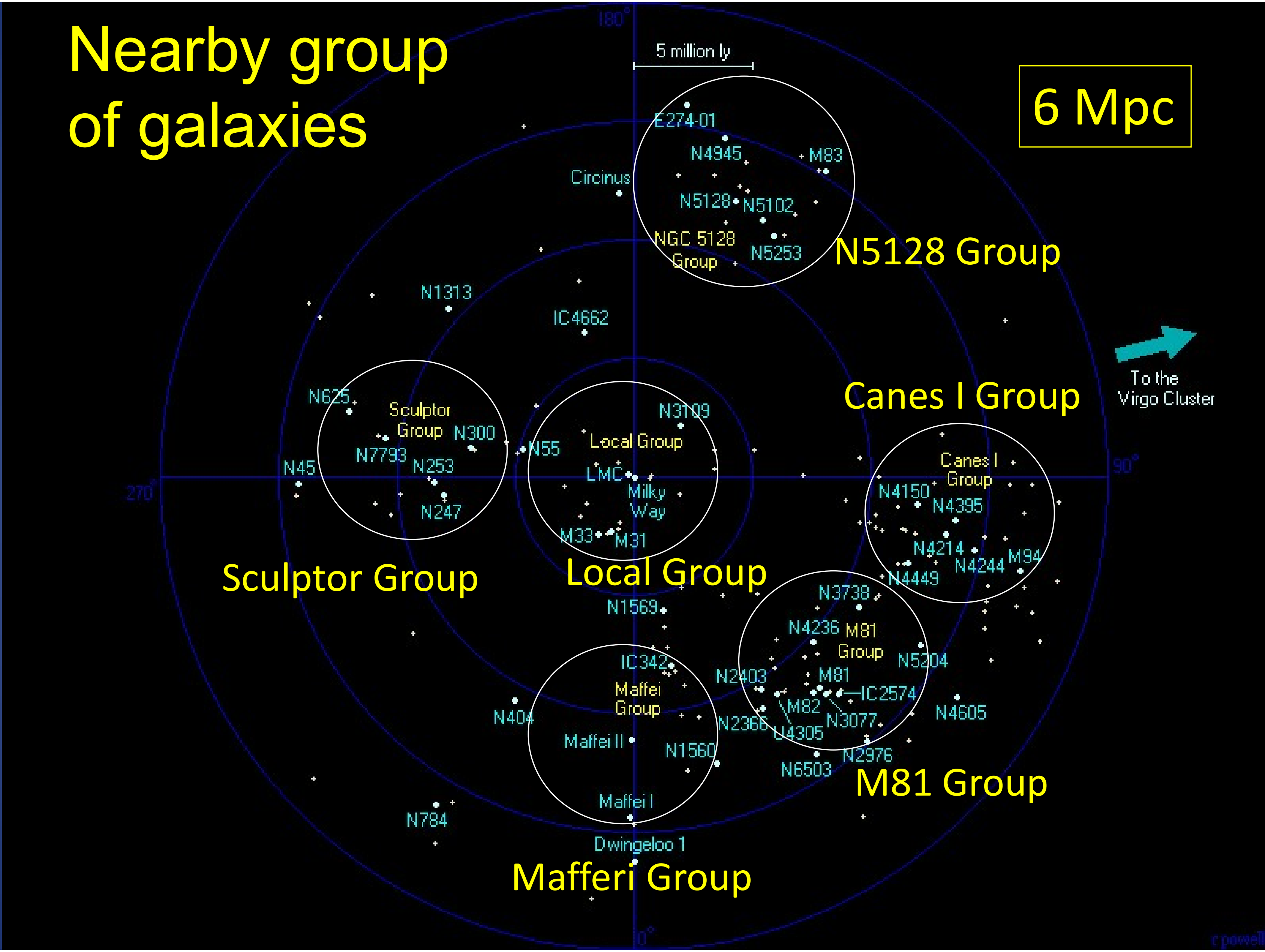

Stellar halos from numerical simulation

～reflecting different merging histories～

Cooper et al. 2010

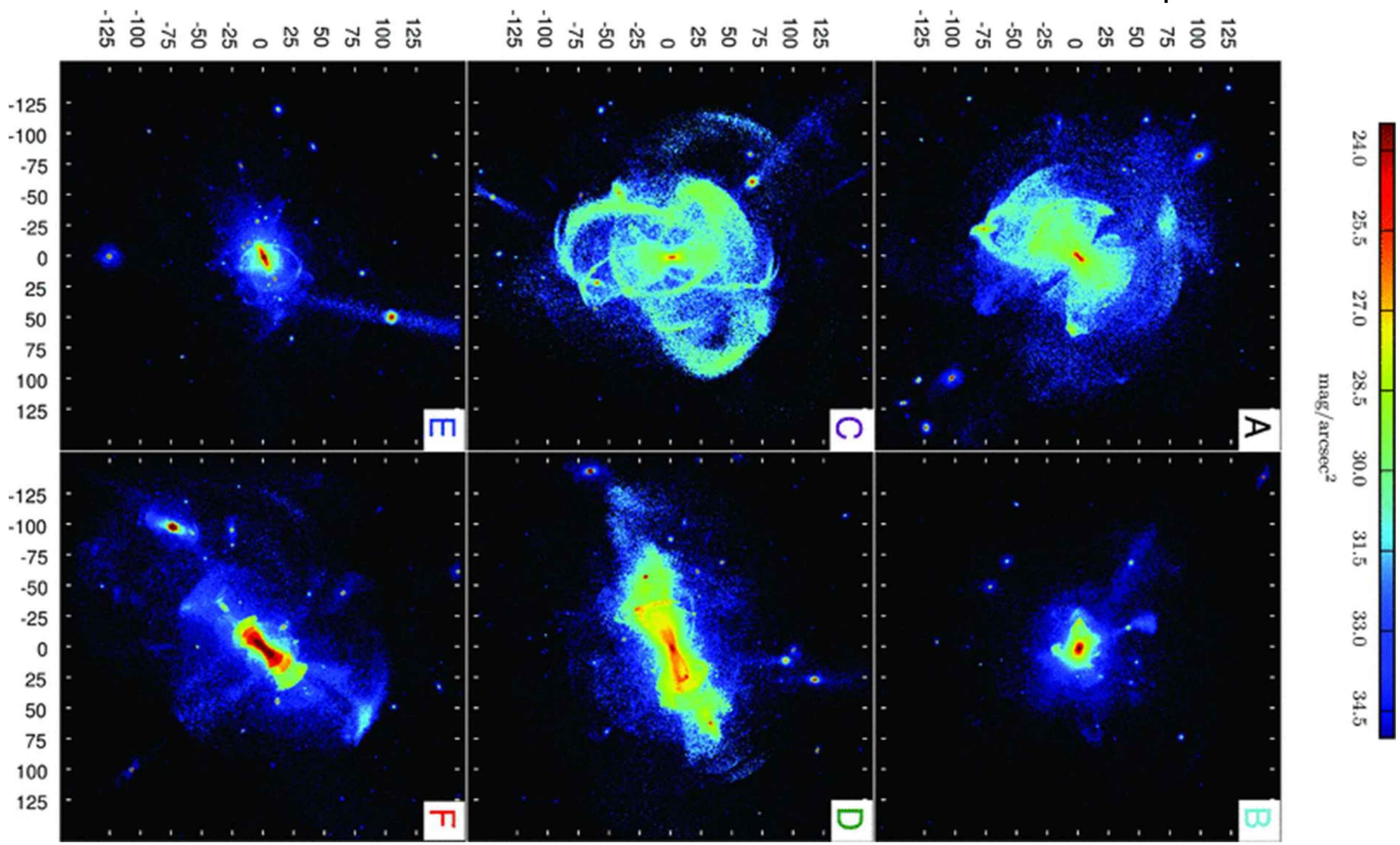

NGC 55 @ Sculptor group D=2.1Mpc

(Tanaka, Chiba, Komiyama, Guhathakurta & Kalirai 2011)

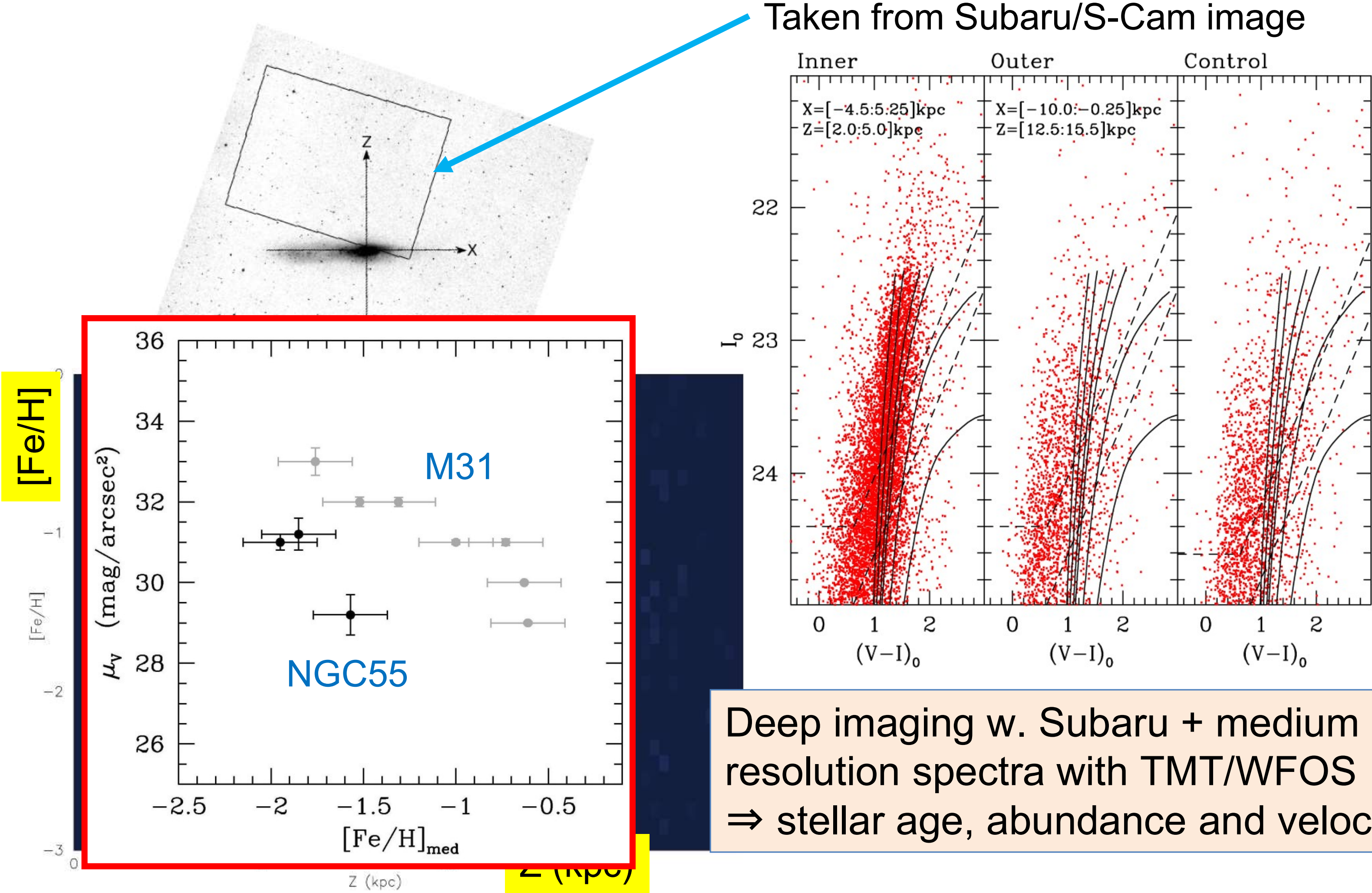

Deep imaging w. Subaru + medium resolution spectra with TMT/WFOS
⇒ stellar age, abundance and velocity

M81 @ M81 group D=3.6Mpc
(Subaru/SuprimeCam: Barker+ 2009)

M81 @ M81 group D=3.6Mpc
(Okamoto et al. 2015)

HSC image

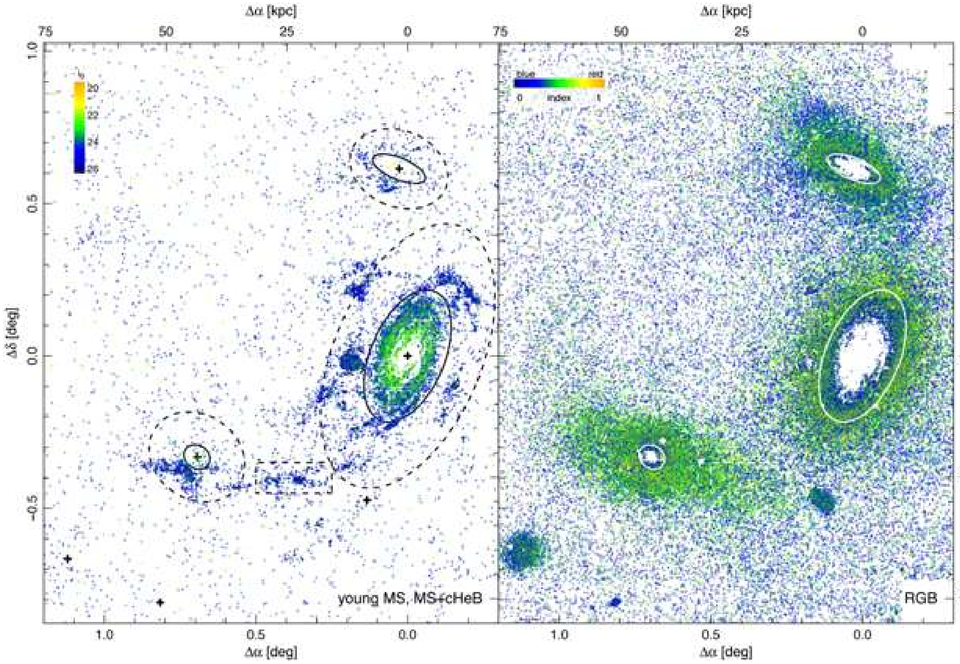

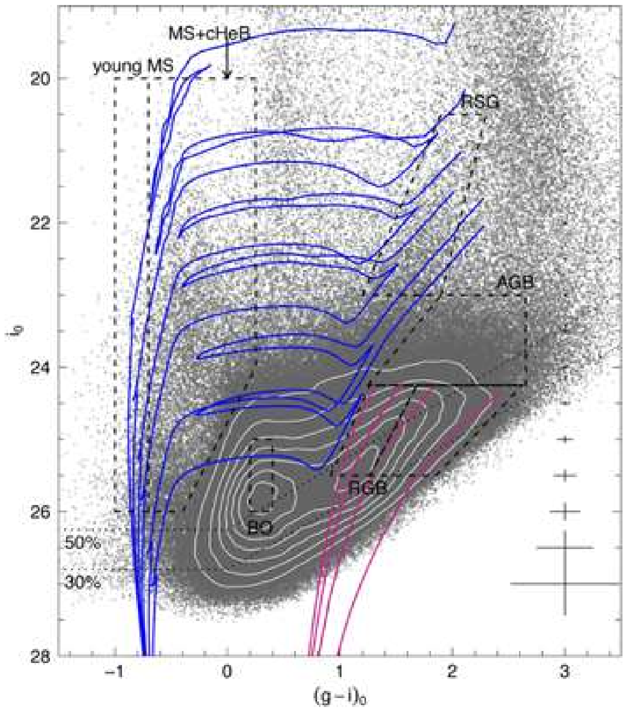

Deep imaging w. HSC + medium resolution spectra with TMT/WFOS
⇒ stellar age, abundance and velocity

Nearby elliptical galaxies
NGC5128 (Cen A)

DEC=-43
D=3.6Mpc

Peng+ 2002 (Blanco T.)

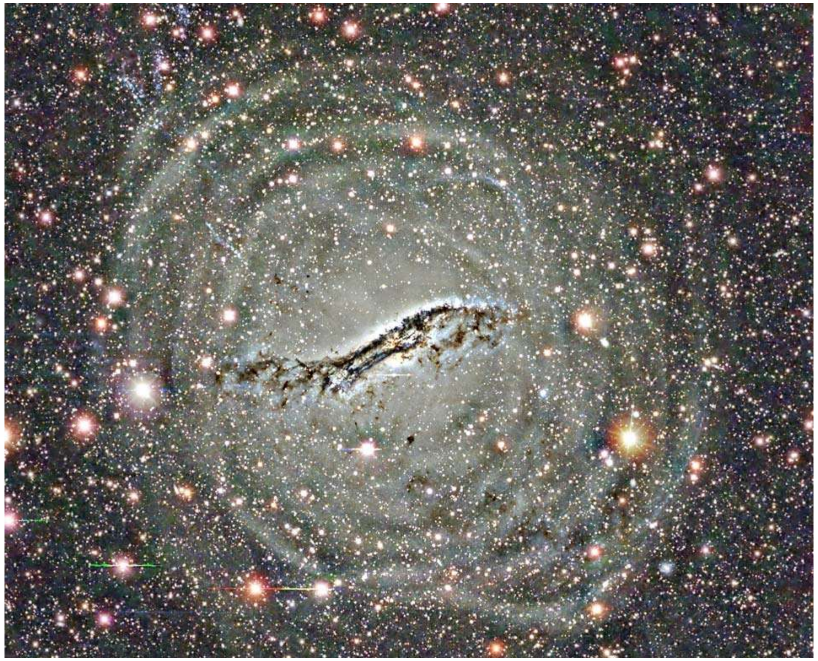

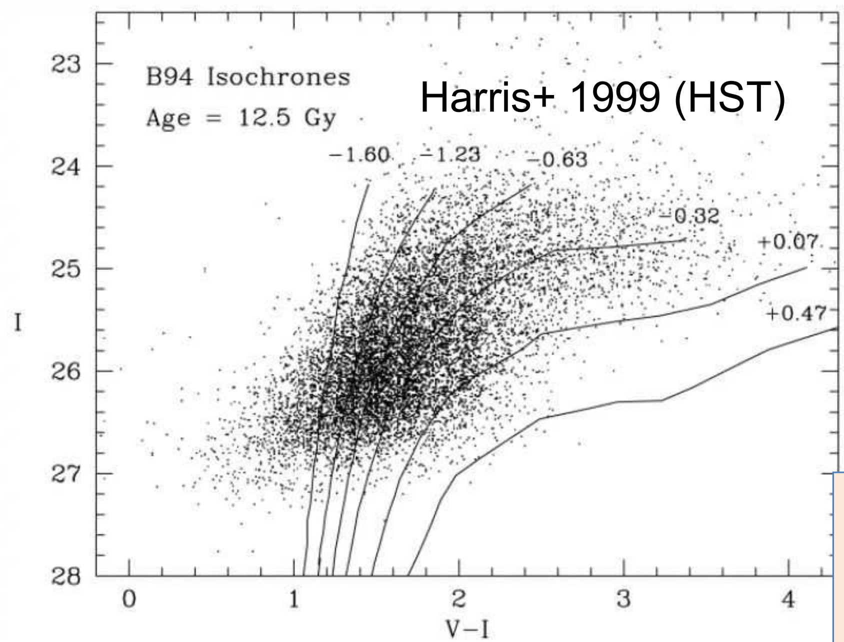

Harris+ 1999 (HST)

Deep imaging + medium
resolution spectra with TMT/WFOS
⇒ stellar age, abundance and velocity

Conclusions

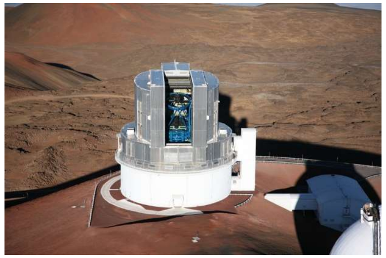

Subaru
HSC
PFS : 2024-
Ultimate:

ALMA

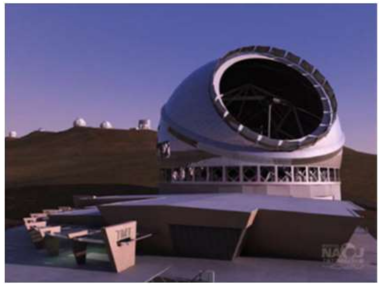

TMT
WFOS
HROS
NIRES
2028?

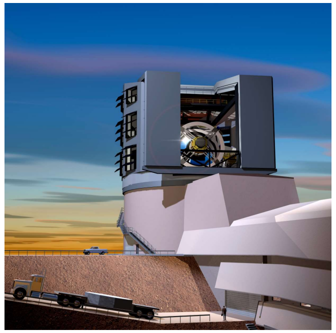

Vera C. Rubin (LSST)
2023-

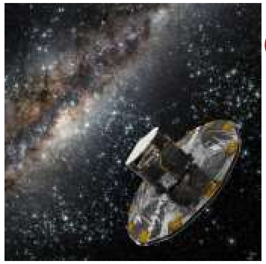

Gaia

JWST
NIRCam
NIRSpec
MIRI
2023-

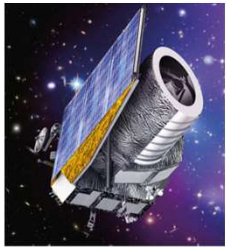

Euclid
YJH
2023-

JASMINE
NIR astrometry
Late 2020

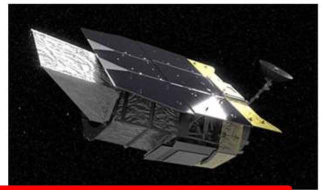

Nancy Grace Roman Space Telescope (WFIRST)
2026-

Very promising future prospects!